This article can be cited before page numbers have been issued, to do this please use: L. Feng, M. Zhang and Z. Fan, *Anal. Methods*, 2024, DOI: 10.1039/D4AY01184H.
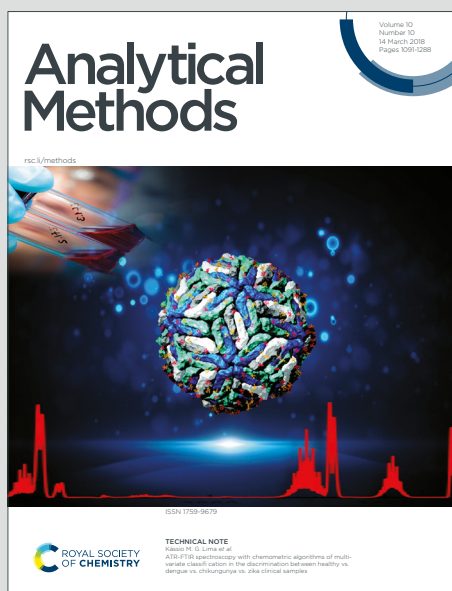
This is an Accepted Manuscript, which has been through the Royal Society of Chemistry peer review process and has been accepted for publication.

Accepted Manuscripts are published online shortly after acceptance, before technical editing, formatting and proof reading. Using this free service, authors can make their results available to the community, in citable form, before we publish the edited article. We will replace this Accepted Manuscript with the edited and formatted Advance Article as soon as it is available.

You can find more information about Accepted Manuscripts in the Information for Authors.

Please note that technical editing may introduce minor changes to the text and/or graphics, which may alter content. The journal's standard Terms & Conditions and the Ethical guidelines still apply. In no event shall the Royal Society of Chemistry be held responsible for any errors or omissions in this Accepted Manuscript or any consequences arising from the use of any information it contains.

ROYAL SOCIETY
OF CHEMISTRY

rsc.li/methods

1

2

Current trends in colorimetric biosensors using nanozymes for detecting biotoxins

(bacterial food toxins, mycotoxins, and marine toxins)

3   Li Feng[a], *, Mingcheng Zhang[b], Zhiyi Fan[c]

4   *[a, b, c] Jiyang College, Zhejiang A&F University, Zhuji Zhejiang 311800, China*

5

6

7

8

9

10

11

12

13

14   * **Corresponding authors**: Li Feng, E-mail: lifeng@zafu.edu.cn

15

16

17

18

19

Analytical Methods Accepted Manuscript

Analytical Methods Accepted Manuscript

20 **Abstract:**

21 Biotoxins, predominantly bacterial food toxins, mycotoxins, and marine toxins, have emerged as

22 major threats in seafood, food, feed, and medicine fields. They have potential teratogenic,

23 mutagenic, and carcinogenic effects on humans, occasionally triggering high morbidity and

24 mortality. One of the apparent concerns relates to the increasing consumption of fast food the

25 demand for processed food without adequate consideration of the toxins they may contain.

26 Therefore, developing improved methods for detecting biotoxins is of paramount significance.

27 Nanozymes, a type of nanomaterials exhibiting enzyme-like activity, are increasingly being

28 recognized as viable alternatives to natural enzymes owing to their benefits, such as customizable

29 design, controlled catalytic performance, excellent biocompatibility, and superior stability. The

30 remarkable catalytic activity of nanozymes has led to their broad utilization in the development of

31 colorimetric biosensors. This has emerged as a potent and efficient approach for rapid detection,

32 enabling the creation of innovative colorimetric sensing methodologies through the integration of

33 nanozymes with colorimetric sensors. In this review, recent development in nanozyme research

34 and its application in colorimetric biosensing of biotoxins is examined with an emphasis on their

35 characteristics and performance. The study particularly focused on the peroxidase (POD) activity,

36 oxidase (OXD) activity, superoxide dismutase (SOD), and catalase (CAT) activity of nanozymes

37 in colorimetric biosensors. Ultimately, the challenges and future prospects of these assays are

38 explored.

39

40 **Keywords:** Nanozymes; Colorimetric biosensing; Biotoxins; Food safety

41

42

Table of Contents

Analytical Methods Accepted Manuscript

Analytical Methods Accepted Manuscript

68   **1. Introduction**

69   Nowadays, there is an emerging concern regarding the rapid monitoring of biotoxin presence in

70   food products[1, 2]. Biotoxins are frequently found in bacteria, viruses, fungi, protozoa, rickettsiae,

71   and infectious substances international polluting feed, food, condiments, seafood, and so forth.

72   Biotoxins pose a risk to public health through the food chain by inducing both chronic and acute

73   toxicity, as well as exhibiting carcinogenic, teratogenic, and mutagenic impacts on human health[3-

74   5]. Certain biotoxin carriers and producers menace human health and pollute the environment; they

75   can lead to crop failures and diminish the quality of agricultural products. Marine are categorized

76   based on their carriers as ciguatoxins, shellfish toxins, mytilotoxin, tetrodotoxins, and others.

77   There exists a wide range of marine toxins, exceeding 1000 different types, with several dozen

78   having been effectively characterized. These toxins have the potential to infiltrate the food chain,

79   leading to human toxicosis and potentially fatal outcomes. For instance, an estimated 750-7500

80   individuals die globally because of shellfish poisoning annually [6]. Bacterial toxins represent a

81   distinct category of biotoxins capable of inducing foodborne illnesses through the inhibition of

82   protein synthesis, leading to neurotoxic effects. The diseases are linked to the impact of bacterial

83   toxins on tissues and are associated with distinct clinical symptoms. The most lethal bacterial toxin

84   associated with food consumption is botulinum toxin, which is created by the *clostridium*

85   *botulinum*. It has been reported that 100 ng of this toxin can be fatal to humans [7]. Mycotoxins are

86   important class of biotoxins that produced as secondary metabolites by fungi, like *Fusarium,*

87   *Aspergillus, Penicillium, Claviceps, Alternaria, Trichoderma, Stachybotrys, Verticimonosporium,*

88   *Chaetomium*, and so forth, under favorable environmental conditions[8]. The pollution can be

89   happening throughout processing, harvesting, transportation, and storage. The International

90   Agency for Cancer Research has classified mycotoxins into distinct categories according to their

91   capacity to trigger cancer in humans. These classifications encompass Group 1, Group 2A, Group

92   2B, Group 3, and Group 4 carcinogens. For example, AFB1 (Group 1 carcinogen aflatoxin B1) is

93   the most toxic and abundant group of mycotoxins. It has been shown to trigger lung carcinoma,

94   hepatocellular carcinoma, colon carcinoma, and gallbladder carcinoma in humans. Liver cancer

95   is caused via AFB1 in around 28.2% of individuals [9].

96   In recent times, biosensors have emerged as a novel method of detection with a broad spectrum of

97   applications for the timely quantitative/qualitative assessment of various biotoxins present in food

98   products[10]. A biosensor is a diagnostic tool that integrates three components: a biorecognition unit

99   (e.g., aptamer, enzyme, antibody, phage, cell, etc.), a transducer and a signal conversion element[11,]

100 [12]. The biorecognition unit is employed to specifically identify the target molecule. The interaction

101 between the target molecule and the recognition unite initiates a series of physicochemical

102 interactions. This reaction is characterized by changes such as light absorption and electrical

103 signals, which form the basis for further signal transduction processes. The transducer, being the

104 most crucial component of the biosensor, is capable of converting the above physicochemical

105 alterations into quantifiable signals, thereby facilitating signal transduction. There exist various

106 types of sensors that can be classified into four main groups based on distinct signal transduction

107 methods: optical sensors, electrochemical sensors, magnetoelectric sensors, and piezoelectric

108 sensors [13, 14]. Among them, the optical sensor plays a crucial role in analyzing the optical signal

109 produced during the integration of the target and the recognition unite, and then through the real-

110 time conversion and signal amplification of the transducer, it will be converted into readable data

111 to realize the quantitative sensing of the target substance. Colorimetric sensing technology is a

112 quantitative optical method that relies on the correlation between the color change of a solution

113 and the concentration of the target analyte. Compared with other optical sensors, the colorimetric

Analytical Methods Accepted Manuscript

114 sensor has the benefits of visualization, low cost, simple operation, and could be coupled with

115 portable substrate, so the practical use is more extensive. This method provide naked-eye sensing

116 abilities (qualitative) and could be incorporated with smartphone imaging (quantitative), making

117 them well-suited for biotoxin presence detection in various foodstuffs [15, 16].

118 Enzymes are regarded as one of the earliest and most frequently utilized biometric components in

119 biosensors. They have a dual role in recognizing the target substance and promoting electron

120 transfer between the substrate, thereby catalyzing the chemical reaction of the specific substrate to

121 induce corresponding signal alterations [17]. Enzymes have the capacity to act as indicators for the

122 identification of particular substances, facilitating the transformation quantities of the target

123 substance into detectable signals for analytical objectives [18]. As a result, the effectiveness of

124 biosensor detection is somewhat dependent on the particular enzymes employed and their

125 individual characteristics. The defects of natural enzymes like difficulty in preservation, high cost,

126 and poor stability limit their more use in biosensors. The rapid advance of enzyme-like

127 nanomaterials (also known as nanozymes) affords an innovative horizon for the choice of suitable

128 signal markers for analyte identification. Nanozymes demonstrate catalytic properties like natural

129 enzymes, allowing them to catalyze effectively even under extreme situations. This attribute

130 expands the potential uses of nanozymes in biosensing applications [19, 20]. The exceptional catalytic

131 efficiency of nanozymes allows them to enhance the color change of platforms, resulting in the

132 generation of light signals upon the colorimetric platforms introduction. The colorimetric

133 biosensor that utilizes nanozymes primarily depends on the catalytic capabilities of the nanozymes

134 to imitate the natural enzymes catalytic functions. This mechanism entails the conversion of a

135 colorless substrate into a colored product through oxidation, enabling visual detection. In contrast

136 to colorimetric biosensors lacking nanozymes, the integration of nanozymes with colorimetric

137   biosensors could serve as a means of signal amplification to a certain extent, thereby enhancing

138   the determination capabilities of biosensors [21]. Nanozymes have the potential to serve as

139   recognition units for target analytes in biosensing systems, and their specific surface area offers

140   more active sites to bind more targets, which could further enhance the sensitivity of colorimetric

141   sensors. Furthermore, nanozymes do not possess inherent light-absorbing properties in

142   colorimetric biosensors. However, upon the addition of a colorimetric substrate, nanozymes

143   exhibit various mimetic enzyme activities that facilitate the catalysis of the substrate reaction,

144   thereby initiating a light signal. This process contributes to signal amplification in colorimetric

145   sensors[22]. As well, the surface properties and specific structure of nanozymes enable them to

146   function as adsorbents for selectively adsorbing target molecules. This capability can enhance the

147   selectivity of the colorimetric sensor.

148   By now, nanozyme-enabled colorimetric biosensors have been broadly employed in food safety

149   analysis owing to the advantages of naked-eye visibility, high sensitivity, easy operation, and

150   portability. However, the applications of nanozyme-enabled colorimetric biosensors in the field of

151   biotoxins analysis have not been specially summarized. Therefore, in this review, we focus on the

152   classification of nanozymes according to the different nanomaterials and offer a detailed

153   description of each type of nanozymes. Moreover, we tried to discuss the construction approach

154   of nanozymes in colorimetric biosensor in terms of catalytic activity, and affords a comprehensive

155   review of the recent research progress of nanozymes in the colorimetric biosensing various

156   biotoxin (mycotoxins, marine toxins, and bacterial food toxins) in food products. Finally, main

157   challenges and prospects of nanozyme-enabled colorimetric biosensors are also deliberated.

Analytical Methods Accepted Manuscript

2. Classification of nanozymes

158

159 Based on their functional activities, nanozymes can be classified into two primary groups: the

160 oxidoreductase family and the hydrolase family. The oxidoreductases predominantly participate

161 in redox reactions and exhibit various activities, including catalase (CAT), oxidase (OXD),

162 superoxide dismutase (SOD), and peroxidase (POD) like functions. Hydrolases play a crucial role

163 in catalyzing hydrolysis reactions and exhibit functions that are analogous to those of proteases,

164 nucleases, and phosphatases, etc[23]. The constituents of nanozymes primarily consist of metals,

165 metal oxides, sulfides, salts, metal-organic frameworks (MOFs), carbon materials, and metal-

166 carbon hybrid nanocomposites [24-26]. Recently, studies on nanozymes have increasingly

167 concentrated on nanomaterials that possess intrinsic catalytic properties, rather than enzymes or

168 catalysts immobilized on nanomaterials. Currently, the majority of published research regarding

169 the nanozymes classification has focused on categorizing them according to their catalytic activity.

170 In order to offer further classification methods for nanozymes, this study emphasis on categorizing

171 them using different nanomaterials and analyzes the fabrication approaches of colorimetric assay

172 based on the various catalytic nanozymes activities.

2.1. Carbon-based nanozymes

173

174 Carbon-derived nanozymes, as a significant constituent of the nanozymes category, refer to

175 carbon-based nanomaterials having enzyme-like catalytic function. Owing to the benefits of

176 environmental friendliness, low cost, good biocompatibility, and easy modification, carbon-based

177 nanozymes are broadly employed in the fields like biosensing, environmental protection, food

178 safety, and disease diagnosis. Nevertheless, unlike other kinds of nanozymes, the synthesis of

179 carbon-based nanozymes mainly relies on a trial-and-error approach. This methodology results in

180 a notable level of uncontrollability in the modulation of the catalytic activity of carbon-based

181 nanozymes. Furthermore, carbon-based nanozymes exhibit a lower degree of substrate specificity

182 compared to other types of nanozymes, primarily due to the absence of substrate binding pockets.

183 Consequently, there is a necessity to advance rational design approaches aimed at addressing this

184 limitation. Extensive study into the characteristics of carbon-based nanomaterials has revealed

185 their significant potential for uses related to catalytic features. The concept of carbon-based

186 nanozymes was simultaneously introduced. The majority of carbon-based nanozymes are

187 documented to own POD-like or OXD-like function. Additionally, to enhance the catalytic

188 properties of these carbon-based nanomaterials, the incorporation of other elemental dopants is

189 often necessary. For instance, N-doped nanocarbon may hold the exceptional catalytic

190 performance[27]. Nevertheless, the synthesis of N-doped carbon nanozymes with a high nitrogen

191 content presents challenges due to the instability of the N element at high temperatures. In 2019,

192 Wei and college utilized polyethyleneimine (PEI) as a source of carbon and nitrogen, alongside

193 montmorillonite (MMT) as a template, to synthesize a carbon-based nanozyme characterized by a

194 high nitrogen content [28]. MMT was dispersed in an aqueous solution, after which the supernatant

195 was subjected to incubation with a polyethyleneimine (PEI) solution. The obtained solution

196 underwent freeze-drying to yield the assembled powder (MP), which was subsequently subjected

197 to carbonization and etching processes to produce nitrogen-doped carbon nanomaterials. This

198 study identified the critical factor, specifically the N doping content, that influences the catalytic

199 performance of carbon-based nanozymes, and thus was of great importance for the development

200 of carbon-based nanozymes with enhanced catalytic performance. Regardless of the significant

201 progress, the most of existing carbon-based nanozymes exhibit only a singular enzymatic activity.

202 Consequently, the development of methodologies to impart dual or multiple enzymatic activities

203 to carbon-based nanozymes is of considerable interest. In light of that, Gao's team used Pluronic

204 F127 as the soft template, and phenol, formalin and melamine as raw materials, to prepare a

205 polymer, which consequently was pyrolyzed to acquire the N-doped carbon [29]. The N-doped

206 carbon N-PCNSs3, prepared under optimal conditions, demonstrated a porous nanosheet

207 morphology, so enabling the substrates to diffuse into the pore to increase reaction performance.

208 Furthermore, the nitrogen content in N-PCNSs3 is significantly greater than that of other

209 comparable materials, which enhances its multi-enzymatic activities and overall catalytic

210 efficiency. As estimated, N-PCNSs3 had the POD-, OXD-, SOD-, and CAT-like activities. It is

211 evident that the catalytic function of carbon-based nanozymes is rest upon the precursor.

212 Consequently, altering the precursor may represent a viable approach for the development of high-

213 performance carbon-based nanozymes. In 2019, Choi and colleagues identified the photo-

214 responsive glucose oxidase (GOx) and POD-like activities of carbon nitride by carbonizing

215 melamine in the KCl and KOH existence [30].

216 Graphene, a subclass of carbon materials, features high conductivity, large surface area, strong

217 thermal stability, and excellent transparency and thus, is deliberated a favorable candidate for

218 preparing carbon-based nanozymes [31]. In 2015, Qu's team found the POD-like function of

219 graphene quantum dots (GQDs) containing of hydroxyl, carboxylic, and carbonyl elements, and

220 thoroughly explore the catalytic mechanism. Following the activity test, it was determined that the

221 carbonyl group serves as the active site and is responsible for determining catalytic activity. The

222 carboxylic group functions to interact with the substrate, while the hydroxyl group is opposite to

223 activity [32]. To the best of our knowledge, this study explained the disturbance of surface functional

224 elements on catalytic function of carbon-based nanozymes for the first time, and thereby will lead

225 further researcher to progress the study of preparation and design of high-performance carbon-

226 based nanozymes. Nevertheless, graphene alone demonstrates minimal catalytic function.

Analytical Methods Accepted Manuscript

227 Graphene, in isolation, demonstrates minimal catalytic activity[33]. To enhance this activity, it is

228 necessary to employ a doping strategy involving other elements such as N, P, B and S.

229 Furthermore, it is essential to optimize the doping methodology to achieve the most effective

230 coordination effects. In 2019, Lee and his colleagues introduced a series of N- and B-doped

231 reduced graphene oxide, like BN-rGO, N-rGO, B-rGO (reaction between melamine and B-rGO),

232 NB-rGO (reaction between H_3BO_3 and N-rGO), and h-BN-rGO (reaction between H_3BO_3,

233 melamine, and rGO)[34]. As expected, the synthesized rGO derivatives exhibited a nanosheet

234 morphology, with the doped elements being uniformly distributed throughout the rGO matrix. This

235 phenomenon may be attributed to the synergistic interaction between N and B, which notably

236 enhanced the electron transmission rate during POD-assisted reaction.

237 2.2. Metal-based nanozymes

238 Metal-based nanozymes are one of the most typical nanozymes owing to their easy synthesis and

239 stable structure. In general, metal-based nanozymes can be categorized into two primary types:

240 single-metal nanozymes and metal alloy nanozymes, which consist of multiple metal constituents.

241 Furthermore, various metal-doped materials, including metal core/shell nanostructures, have been

242 successfully synthesized [35]. These nanozymes show diverse shapes, like nanowires, nanoflowers,

243 nanoparticles (NPs), nanosheets, and nanospheres. Various shapes can exhibit distinct catalytic

244 characteristics. Among them, precious metal NPs like gold, silver, platinum, and palladium are

245 commonly exploited in the determination of bacterial food toxins, mycotoxins, and marine toxins.

246 The synthesis techniques of metal-based nanozymes comprise photochemical, high-temperature

247 reduction, and mediated growth methods. In the experiments concerning nanozyme-assisted

248 analytes sensing, the reduction technique is primarily utilized. For instance, PtNPs were produced

249 using polyvinylpyrrolidone (PVP) as a stabilizing agent sodium and citrate as a reducing agent,

250 whereas AgNPs were prepared using potassium hydroxide and L-tyrosine as raw materials, which

251 all have excellent peroxidase function[36, 37]. In addition to exhibiting single-enzyme-like activity,

252 certain metal-based nanozymes may also demonstrate multi-enzyme-like activity. For instance,

253 peroxidase-like and oxidase-like IrNPs were made-up based on PVP and $IrCl_3$-$3H_2O$ as raw

254 materials through alcohol reduction technique[38, 39]. The combined influence of these two activities

255 enhanced the sensitivity and selectivity of the nanozyme. Due to the synergistic interactions among

256 each component, bimetallic nano-alloys frequently exhibit enhanced catalytic behavior. Recently,

257 bimetallic nanocomposites received significant attention owing to their distinctive synergistic

258 effect and multifunction, and are extensively exploited in catalytic field. The Au-Pt nanozyme

259 demonstrated superior peroxidase-like activity compared to the Au nanozyme alone and exhibited

260 greater stability over time than horseradish peroxidase (HRP). This phenomenon can be attributed

261 to the disparity in electronegativity between Pt and Au, which facilitates the migration of electrons

262 from Pt to Au. This transfer enhances the surface electron density of Au, thereby augmenting its

263 catalytic activity [40]. To mitigate costs, the copper (Cu) as an element was employed in the

264 synthesis of bimetallic nanocomposites. Ramanathan et al. investigated the process of electroless

265 deposition to facilitate the in-situ growth of Cu NPs on the surface of cotton fabrics [41]. The obtained

266 cotton fabrics were then submerged in water solution having $AgNO_3$ or $HAuCl_4$ or $PdCl_2$ or

267 H_2PtC_{l6} to prepare bimetallic nanoparticles, like Cu-Ag, Cu-Au, Cu-Pd and Cu-Pt. Cu-Pt NPs

268 displayed the excellent POD-like function and highest catalytic rate. Despite the extensive research

269 conducted on metal-based nanozymes, the tendency to aggregate and the toxicity associated with

270 certain heavy metals pose significant limitations to their potential applications [42].

Analytical Methods Accepted Manuscript

2.3. Metal oxidize-based nanozyme

271 As well to metal-based nanozymes, newly, metal oxide/sulfide/salt-derived nanozymes have

273 gathered higher considerable attention because they enjoyed the merits of simple preparation steps,

274 low cost, and distinctive magnetic/dielectric/optimal features [43, 44]. Considering our understanding,

275 the frequently applied techniques mainly included sol–gel, hydrothermal reaction, atomic layer

276 deposition and air pyrolysis. Through adjusting the surface groups, structures, and categories, the

277 catalytic behavior of nanozymes along with functionality and stability can be readily controlled.

278 The pioneering research on nanozymes was documented via Yan in 2007. This study revealed that

279 Fe_3O_4 NPs exhibited POD-like activity for the first time[45]. Engaging TMB, OPD and

280 diaminobenzidine (DAB) as substrates, Fe_3O_4 NPs catalyzed oxidation of them producing blue,

281 brown and orange color, on the basis of which Fe_3O_4 NPs revealed POD-like function.

282 In addition to Fe_3O_4 NPs, V_2O_5 nanocomposites were also typically used to synthesis nanozymes,

283 and till now, V_2O_5 enjoying OXD-, POD-, and dual-enzyme (GOx and POD)-like function with

284 1D and 2D morphologies are introduced. The primary instance of V_2O_5 with POD-like

285 performance was documented by Tremel's team research [46]. Initially, $KBrO_3$ and $VOSO_4$ were

286 combined, after which HNO_3 was slowly added to achieve a pH of 2.0. Following this, thermal

287 treatment was conducted at 180 °C for 24 h to synthesize V_2O_5 nanocomposites. In another study,

288 Doong et al exploited the bulk V_2O_5 powder as the raw material, and using DMF to separate bulk

289 V_2O_5[47]. The V_2O_5 nanosheets demonstrated significant oxidative activity, effectively catalyzing

290 the oxidation of TMB to oxTMB. In 2023, Li et al. utilized the reaction between $KBrO_3$ and

291 $VOSO_4$ to synthesize 2D V_2O_5 by optimizing the reaction conditions [48]. The resulting 2D V_2O_5

292 exhibited superior POD-like activity compared to V_2O_5 with other morphologies.

293   MnO_2 was also typically used to develop nanozymes with CAT-, POD-, OXD-, GOx- and SOD-

294   like activities. For instance, Han and colleagues used BSA as soft template to controllably produce

295   2D MnO_2 nanozyme[49]. Actually BSA with rich-NH_2 and -COOH elements could efficiently fixe

296   Mn^{2+} in its molecular structure to generate $Mn^{2+}@BSA$. Upon the addition of NaOH, Mn^{2+} present

297   in the $Mn^{2+}@BSA$ complex was initially converted into MnO(OH). This intermediate

298   subsequently underwent oxidation by O_2, ultimately resulting in the formation of MnO_2. As

299   anticipated, the synthesized MnO_2 under alternative conditions exhibited an irregular flocculent

300   morphology, highlighting the significant influence of BSA.

301   To sum up, metal oxide-based nanozymes, like peroxidase-like V_2O_5, GeO_2, TiO_2, Fe_3O_4, and

302   oxidase-like MnO_2 are also employed in the determination of various toxins. Nevertheless, the

303   unmodified metal oxide-derived nanozymes might display poor stability and other challenges [50].

304   Consequently, some researchers will alter specific components within the metal oxide to enhance

305   its detection efficacy.

2.4. MOF-based nanozymes

307   MOFs are crystalline materials characterized by a periodic network structure that arises from the

308   self-assembly of organic components, typically organic ligands such as pyridine or carboxylic

309   acids, in conjunction with metal clusters or metal ions, predominantly comprising transition metal

310   ions like Fe^{2+}, Zn^{2+}, and Cu^{2+} [51, 52]. MOFs are a class of nanomaterials that have garnered

311   significant interest in recent years due to their advantageous characteristics, including a high

312   specific surface area, a porous network structure, and tunable chemical properties [53]. The poor

313   selectivity is prevalent among numerous nanozymes; therefore, it is essential to conduct a thorough

314   investigation into the factors contributing to the high selectivity observed in natural enzymes and

315   to incorporate these insights into the development of nanozymes. Similarly, when utilizing MOF-

316 based nanozymes in vivo, it is imperative to assess their cytotoxicity and biosafety to confirm that

317 they do not pose any harm to the organism. According to their synthesis approaches, MOF-based

318 nanozymes could be divided into chemically modified MOF, pristine MOF, MOF derivatives and

319 MOF-based composites [54].

320 The coordination binding sites of the metal centers within MOFs are often obstructed by the

321 organic moieties, leading to diminished catalytic activity. Therefore, it is imperative to explore

322 novel strategies to address this issue and enhance the catalytic performance of the unmodified

323 MOF. Strategies have been established to augment their catalytic performance, like assembly of

324 metal nanoparticles, surface modification of MOFs, metal oxides, and other constituents in MOF

325 [55]. The Fe_3O_4@MIL-100(Fe) composites were effectively synthesized using an in-situ growth

326 technique, which involved the incorporation of Fe_3O_4 NPs within the MIL-100 framework. The

327 catalytic potential of these MOF composites for photo-Fenton reactions was subsequently

328 investigated [56]. Research has also been conducted on the synthesis of AuNPs@MIL-101

329 composites through the hydrothermal deposition of AuNPs onto the MIL-101 MOF. This

330 composite material exhibits catalytic properties for the oxidation of ascorbic acid, which can be

331 utilized in conjunction with an electrochemical sensor for the detection of microcystin-LR in water

332 samples [57]. Both rGO and TiO_2 have been revealed to couple with MIL MOFs to improve their

333 catalytic function[58, 59]. In addition, MOFs could also be applied as templates or precursors to

334 provide a series of MOF derivatives, for example carbon materials, metal oxides, metals, and so

335 on, owing to their modifiable structures. For instance, by calcining the precursors of Fe-ZIF-67

336 and Fe-ZIF-8 at high temperatures, a Fe-N-C nanzyme with POD-like function was achieved,

337 which exhibited good performance [60].

3. Colorimetric biosensor using nanozymes activity

As is well known, colorimetric biosensing relies on the correlation between the extent of color alteration in the platform and the level of the analyte substance to enable quantitative determination. The alteration in substrate color is dependent on the catalytic function of the enzyme. Nanozymes typically facilitate the conversion of a colorless substrate into a colored one through their inherent enzyme-like properties. For instance, nanozymes exhibit the ability to induce color changes in various substrates, including OPD (o-phenylenediamine), TMB, ABTS, and other chromogenic substrates, enabling colorimetric recognition. Recently, the most research endeavors concerning the catalytic capabilities of nanozymes have primarily concentrated on imitating oxidoreductase characteristics, specifically those associated with OXD, POD, CAT, and SOD functionalities [61]. Some previous studies have explored hydrolytic enzyme mimics, however, the focus has shifted towards the oxidoreductase-imitating capabilities of nanozymes, particularly in the context of colorimetric sensing. This section primarily examines the development strategies and advancements in employment colorimetric nanoprobes that leverage the oxidoreductase-like properties of nanozymes. In recent years, there has been a growing interest in the integration of biosensors with innovative nanomaterials, and nanozymes are broadly exploited in colorimetric recognizing platforms owing to their superior stability and exceptional catalytic characteristics. From one perspective, nanozymes have the potential to serve as biorecognition units for analytes in biosensing applications, as they offer a large specific surface area that can render numerous active sites for binding multiple targets, which in turn can effectively boost the colorimetric sensors sensitivity [62, 63]. Furthermore, nanozymes lack inherent light-absorbing characteristics in colorimetric nanoprobes. However, upon the addition of a colorimetric platform, nanozymes exhibit diverse simulated enzyme performances that facilitate the catalysis of the surface reaction,

361 thereby initiating a light signal. This mechanism enables nanozymes to contribute to signal

362 enhancement within colorimetric probes [22]. Additionally, the distinct building and interface

363 characteristics of the nanozymes enable them to function as adsorbents for selectively capturing

364 the desired molecules. This capability could enhance the colorimetric assay selectivity. More

365 importantly, nanozymes play a crucial role in inducing a color change in the substrate as part of

366 the catalytic process. This transformation enables the conversion of the concentration or amount

367 of the desired molecules into visible hue indicators, facilitating the naked eye detection of signal

368 variations through colorimetric sensors.

2.1. POD-like activity

369

370 Peroxidase could catalyze the reaction in the peroxides existence like ROOH and as H_2O_2 redox

371 substrates and electron acceptors, changing them to oxidation and H_2O products [64]. The

372 nanozymes' POD mimetic system exhibits ping-pong mechanism and Michaelis-Menten kinetics

373 similar to those observed in the catalytic behavior of natural peroxidase enzymes [61]. The ping-

374 pong mechanism is defined by the enzyme's alternating transition between its initial conformation

375 and an altered state. This process involves the enzyme releasing the initial product upon binding

376 with the initial substrate in its base state, transitioning to the altered form, and reverting to the

377 original conformation upon binding with the second substrate to release the subsequent product [65].

378 In contrast to the OXD mimetic activity, the POD mimetic system requires the presence of H_2O_2.

379 H_2O_2 serves as a natural scaffold toward POD, and the nanozymes facilitate the breakdown of the

380 O–O bond in H_2O_2 into (·OH) with significant oxidation potential. The resulting ·OH species can

381 subsequently oxidize various colorimetric substrates, including OPD, ABTS, TMB, and other

382 similar compounds [22]. The production of ·OH in processes mimicking peroxidase enzyme activity

383 has been documented through two pathways. One pathway involves the Fenton reaction, where

Analytical Methods Accepted Manuscript

384   Fe^{2+} reacts with H_2O_2 to produce ·OH and hydroxides (OH^-). The Haber-Weiss reaction as a

385   second pathway can catalyze superoxide ($·O^{2-}$) via iron ions and H_2O_2 leads to the generation of

386   ·OH [66].

387   The emerging trend in analytical chemistry involves utilizing nanozymes with inherent peroxidase-

388   like activity in conjunction with colorimetric biosensors for the purpose of detecting specific target

389   substances. This approach is using catalytic color development concept through nanozymes.

390   Graphite-like carbon nitride (g-C_3N_4) nanosheets exhibit properties similar to POD enzymes with

391   notable stability. Notably, the functionalization of g-C_3N_4 with heteroatoms has been shown to

392   substantially improve its POD-like activity. In this regard, Fu's group activated g-C3N4 with Pd

393   NPs for the improvement of its enzyme-catalyzed performance and loaded the heteroatom-

394   activated g-C_3N_4 with Fe_3O_4 [67]. A magnetic platform consisting of Fe_3O_4/Pd NPs supported on g-

395   C_3N_4 was developed to enhance POD-like activity and utilized for immobilizing different natural

396   enzymes, aiming to achieve material reusability and mitigate optical nanozymes interference

397   caused by scattering in colorimetric sensors. Using Fe_3O_4/Pd NPs/g-C_3N_4/GOx, a colorimetric

398   probe was developed for the determination of glucose. There was no detectable evidence at 652

399   nm once TMB, glucose, and Fe_3O_4/Pd NPs/g-C_3N_4 without GOx were existent, indicating that

400   Fe_3O_4/Pd NPs/g-C_3N_4 does not exhibit inherent GOx-like function. The alteration in TMB hue was

401   observed only when Fe_3O_4/Pd NPs/g-C_3N_4/GOx, TMB, and target were co-present.

402   In another study, Li et al. [68] produced S- and N-doped carbon-loaded POD-like FeCoZn triatomic

403   catalysts stemmed from ZIF-8 by taking benefit of two properties, specifically, that MOFs could

404   efficiently mitigate the issue of single-atom catalyst agglomeration and the potential of dispersing

405   multiple metal atoms to boost the efficiency of single-atom nanozymes. A colorimetric nanozyme

406   using dual-channel assay was developed by integrating FeCoZn-TAC/SNC with a sensor array,

407   aimed at differentiating food preservatives (Figure 1). The FeCoZn-TAC/SNC nanozymes exhibit

408   POD-like activity, facilitating the color development reactions of TMB and OPD to yield green

409   and yellow products, respectively. The food preservatives can adhere to the nanozyme surface via

410   hydrogen bonding and π-π stacking interactions. The diverse levels of interaction noted between

411   FeCoZn-TAC/SNC and different food preservatives led to a reduction in the catalytic efficiency

412   of the nanozymes. Consequently, this occurrence resulted in varying degrees of color signals,

413   which serve as the fundamental mechanism for discriminating among the preservatives. According

414   to this principle, the colorimetric reaction profiles of various preservatives exhibit variations.

415   Through linear discriminant analysis, a 100% accuracy rate was attained during the cross-

416   validation of seven food preservatives. This result indicates that the sensor array adeptly

417   distinguished seven varieties of food preservatives even at low concentrations.
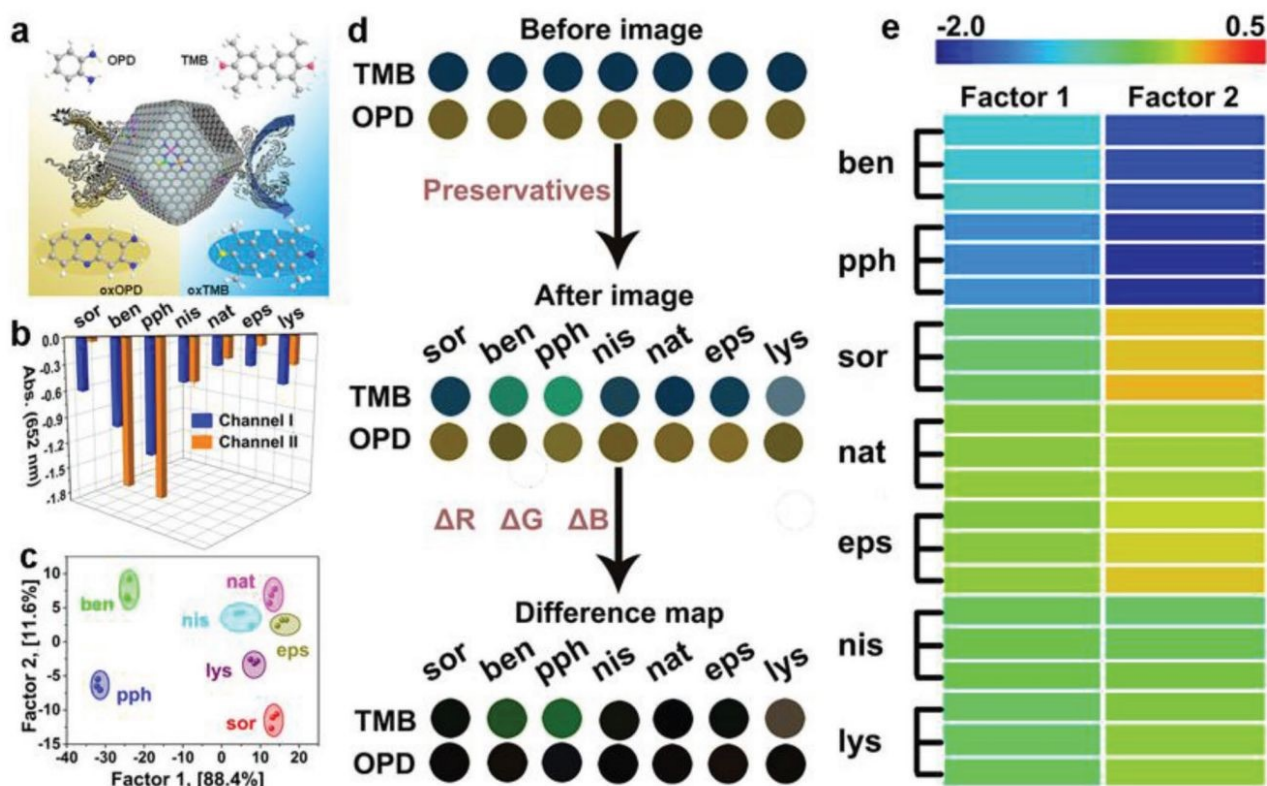
418

419

420   **Figure 1.** Schematic drawing of fabricating a colorimetric biosensor using two-channel array on

421   the basis of the POD-like function of nanozymes for discriminating food preservatives. Reprinted

422   with permission from Ref [68].

2.2. Oxidase-like activity

424   Oxidases have the ability to facilitate the substrates oxidation (such as electron donors) in the

425   existence of molecular oxygen or other oxidants (such as electron acceptors), leading the

426   production of oxidation products along with H_2O, H_2O_2, or O^{2-}. Currently, a variety of nanozymes

427   have been identified to exhibit oxidase-like activity. Massimiliano and colleagues discovered that

428   gold nanoparticles (Au NPs), even when not loaded with protective agents, exhibited enhanced

429   catalytic activity. Bare Au NPs exhibited the capability to catalyze the production of H_2O_2 and

430   gluconate from glucose in the O_2 presence. In contrast, colloidal particles of Ag, Cu, Pt, and Pd

431   did not demonstrate comparable activity under identical conditions [69]. Thereafter covalent organic

432   frameworks, metal-organic frameworks, carbon-derived nanozymes, and other nanozymes have

433   been identified to possess OXD-like activity [70-73]. The colorimetric biosensors can be developed

434   by utilizing the color change resulting from the catalytic process of oxidases, where the in situ

435   production of superoxide radicals and hydrogen peroxide oxidizes colorless substrates into colored

436   products [74]. To some extent, the OXD mimics are considered more appropriate for biochemical

437   analysis compared to the POD mimics due to their ability to function without the need for H_2O_2 in

438   the catalytic procedure. Additionally, the reaction situations for the enzyme mimics are simpler

439   and more direct. Nevertheless, Singh and colleagues determined that nanozymes possessing OXD-

440   like activity have the capability to trigger molecular oxygen conversion into reactive oxygen

441   species like singlet oxygen, oxygen radicals, and hydroxyl radicals during the catalytic mechanism,

442   which can be effectively utilized for the oxidation of diverse substrates[75-77]. This results in a lack

443 of specificity in the catalytic activity of the nanozymes during the substrate process. In order to

444 address this issue, they developed a biomimetic approach utilizing MOF materials. Through the

445 manipulation of MOF crystal growth in the Z direction, researchers successfully synthesized

446 ultrathin nanosheets of Mn-UMOF using benzene dicarboxylic acid and triethylamine. The

447 presence of the robust donor ligand triethylamine and the bridging ligand benzene dicarboxylic

448 acid in Mn-UMOF leads to an increased density of active sites and enhanced substrate binding

449 properties, particularly for electron unsaturated, when compared to the bulk Mn-BMOF.

450 Additionally, Mn-UMOF could better catalyze the substrates oxidation like amplex red (AR),

451 ABTS, and TMB without the any external oxides addition [78].

452 In another study, Zhang's team established an innovative technique that can selectively identify

453 thiophanate-methyl [79]. A Cu-doped carbon nanozyme, denoted as Cu@NC, was developed with

454 Cu serving as the active center site. The thiocarbamide-like and ethylenediamine-like buildings in

455 the target analyte, thiophanate-methyl exhibit a robust affinity for metal ions. This property enables

456 thiophanate-methyl to selectively interact with Cu@NC in the existence of other pesticides,

457 leading to a significant reduction in the catalytic performance of the nanozyme and facilitating

458 colorimetric detection (Figure 2). The researchers also examined the specificity of the colorimetric

459 sensor and revealed that thiophanate-methyl had a direct and specific inhibitory effect on the OXD

460 performance of Cu@NC nanozymes. To examine the mechanism through which the nanozymes

461 activity is inhibited, experiments were carried out. These experiments revealed a reduction in the

462 nanozymes catalytic activity after pre-incubating the target molecule, thiophanate-methyl, with

463 Cu@NC. Subsequently, the thiophanate-methyl was introduced to the chromogenic substrate.

464 Upon the introduction of thiophanate-methyl into the conventional system consisting of TMB and

465 Cu@NC, it was observed that the catalytic activity remained unaffected. This suggests that the

Analytical Methods Accepted Manuscript

466 decrease in Cu@NC activity caused by thiophanate-methyl is a result of its direct interaction with

467 Cu@NC, rather than from enhancing the reduction of oxTMB. Additional inhibitory elements

468 were subsequently examined, and it was lastly found that TM can be fixed onto the Cu@NC

469 interface via π-π stacking interactions and attached to its metal sites to suppress its catalytic

470 function.

471

Direct and Specific Nanozyme Inhibition
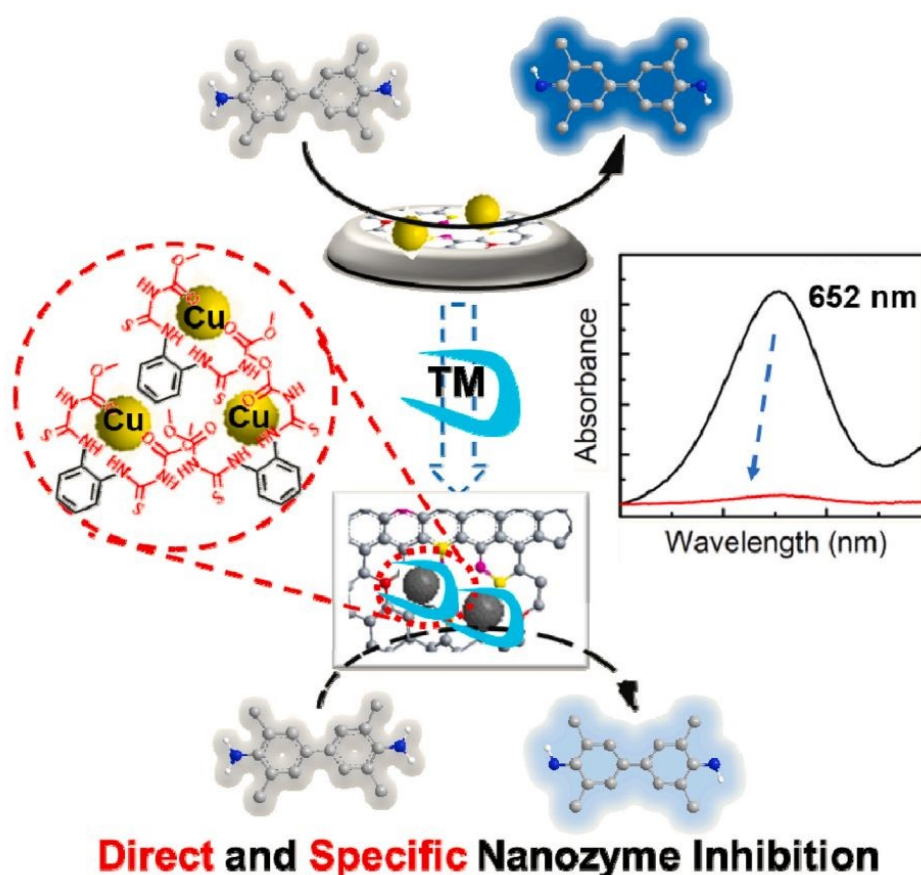
473 **Figure 2.** Diagram illustrating the development of a colorimetric nanoprobe utilizing the OXD-

474 like properties of nanozymes for the precise identification of thiophanate-methyl. Reprinted with

475 permission from Ref [79].

476   CeO$_2$ nanoparticles demonstrate remarkable mimetic activity similar to oxidase enzymes, enabling

477   the catalysis of TMB color progress in the absence of hydrogen peroxide. In this regard, Jia's group

478   developed a multifunctional incorporated portable colorimetric detecting substrate for the

479   determination of bisphenol A [80]. As depicted in Figure 3, the experimental configuration utilized

480   the CeO$_2$@ZIF-8/Apt nanoprobe both the signal generation unit and recognition component.

481   Sodium alginate hydrogel tubes were employed to contain the TMB and catalytic reaction buffer

482   as the reaction medium. The hydrogel containing the TMB platform was attached to the top of the

483   tube, while the signal probe was placed at the base of the tube. Following the introduction of the

484   sample and subsequent mixing with the signal probe, the Apt molecules on the signal probe

485   dissociated and attached to the target, which resulted in the triggering of the OXD activity from

486   the CeO$_2$@ZIF-8. Upon completion of the reaction process, photographs of the reaction solution

487   were taken using a smartphone subsequently uploaded to a color analysis based on the RGB app.

488   This method was employed to quantitatively evaluate the target object.

$$\Delta C = \sqrt{(\Delta R)^2 + (\Delta G)^2 + (\Delta B)^2}$$
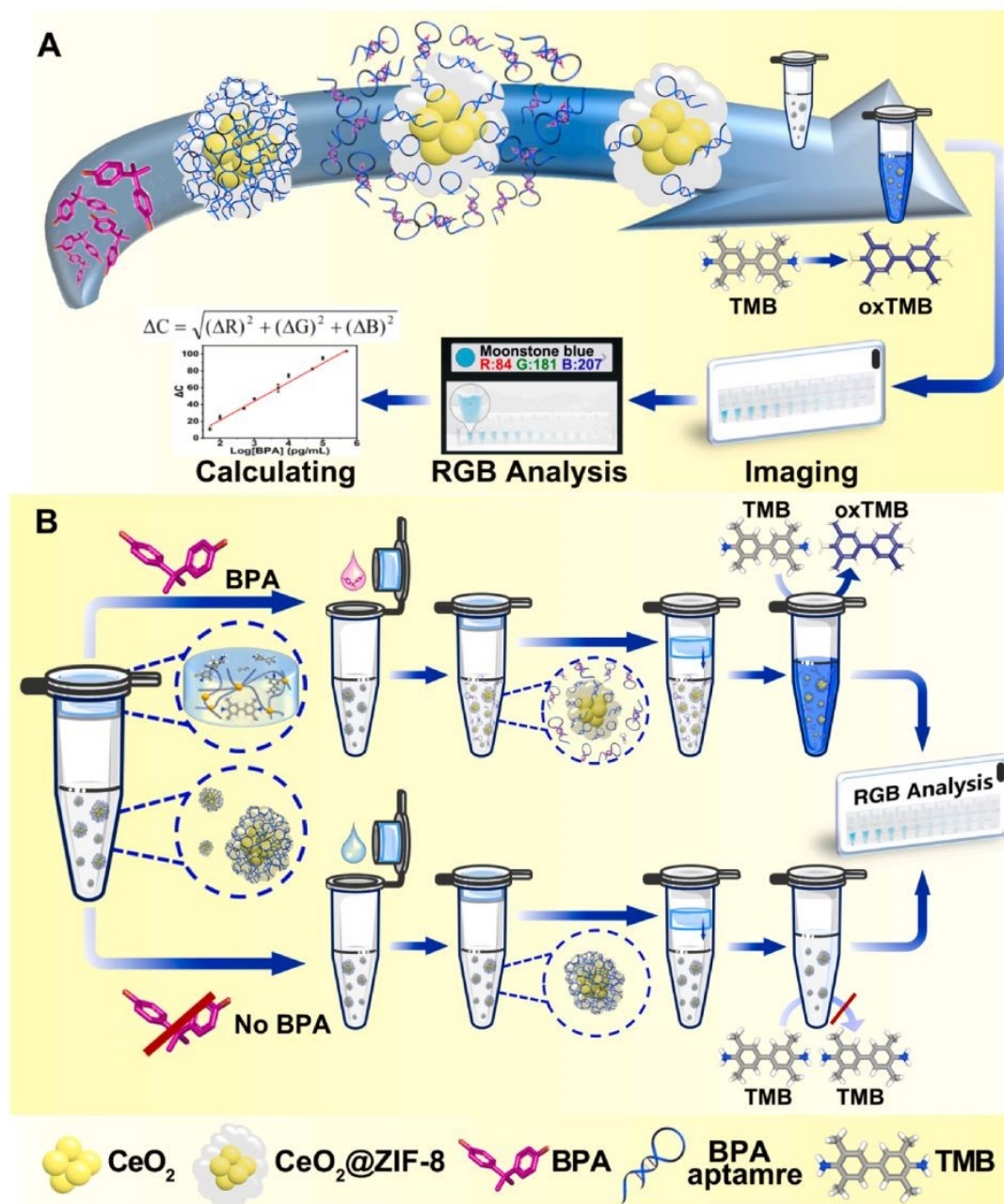
Figure 3. (A) Diagram description of the fabrication and the OXD-like properties of CeO_2@ZIF-8/Apt nanoprobes. (B) The sensing mechanism of one-pot portable testing substrate for bisphenol A determination. Reprinted with permission from Ref [80].

2.3. Catalase-like activity

494 The catalase enzyme facilitates the degradation of hydrogen peroxide into oxygen and water. The

495 catalase-like properties of NPs were first reported in amine-terminated PAMAM dendrimers that

496 encapsulated gold nanoclusters, which were observed in both physiological and acidic

497 conditions[81]. Likewise, several nanozymes-like manganese oxide (Mn_3O_4) nanoparticles, platinum

498 nanoparticles, and cerium oxide nanoparticles are defined to display the catalase-like activity. The

499 molecular-level investigation of the catalase-like behavior of nanozymes explores mechanisms

500 involving bi-hydrogen peroxide association, base-like dissociation, or acid-like dissociation [82].

501 The bi-hydrogen peroxide mechanism has been identified as the most appropriate explanation for

502 the catalase-like activity in nanozymes, particularly in the case of cobalt (II, III) oxide (Co_3O_4)

503 nanoparticles. The catalase-like activity of cerium oxide nanoparticles involves the oxidation of

504 hydrogen peroxide on the nanoparticles' surface to form oxygen. This process leads to the

505 reduction of cerium oxide to H_2-ceric oxide. Subsequently, H_2-ceric oxide reacts with another

506 hydrogen peroxide molecule, resulting in the production of water[83]. Further, Zhang et al. illustrated

507 the catalase-like function of iron-based single atom nanozymes (Fe-SANzymes) considered via

508 obviously exposed edge-hosted defective Fe\N_4 atomic sites[84]. The mechanistic investigation

509 demonstrates that defects facilitate a substantial charge transfer from the Fe atom to the carbon

510 matrix. This process activates the central Fe atom, enhancing its interaction with hydrogen

511 peroxide and simultaneously weakening the O\\O bond.

2.4. Multi-enzyme-like activity

513 Nanozymes with CAT-like function are frequently employed to eliminate extra naturally

514 happening reactive oxygen hydrogen peroxide, which is somewhat close to POD enzymes.

515 Nevertheless, nanozymes typically lack the capability to oxidize substrates to enable hue advance.

516 Consequently, it is less frequent to depend solely on the nanozymes in terms of the CAT activity

517 for the fabrication of colorimetric nanoprobes. Superoxide dismutase is a metalloenzyme with

518 antioxidant properties found in various organisms, capable of enabling the dismutation of reactive

519 superoxide anion radicals into O_2 and H_2O_2. SOD enzymes like CAT enzymes were frequently

520 employed to neutralize surplus reactive oxygen classes, playing a pivotal role in body's oxidation

521 and antioxidant equilibrium. The catalytic mechanism of SOD enzymes primarily entails the

522 protonation of superoxide anion ($O2^{\cdot -}$), which in turn protonated by water to produce OH^- and

523 $HO2^{\cdot}$ radicals. Nanozymes with $O2^{\cdot -}$ scavenging capability are deliberated to be favorable

524 substitutes to natural SOD enzymes. If nanozymes demonstrate multiple simulated enzyme

525 functions simultaneously, like SOD, OXD, and POD, the dominant activity is expected to be the

526 SOD enzyme activity. This activity is influenced by factors like environmental pH, surface ions,

527 and nanomaterial structure [85]. Currently, the majority of reported nanozyme activities focus on

528 POD and OXD activities, with limited research on mimicking SOD activity. Moreover, given that

529 the primary purpose of the SOD enzyme is to preserve redox equilibrium in cells and mitigate

530 oxidative stress, a significant portion of research endeavors focusing on nanozymes with SOD-

531 mimetic characteristics are primarily directed towards mitigating inflammation. In contrast, there

532 is a conspicuous lack of research investigating the employment of SOD nanozymes in colorimetric

533 recognizing methodologies. Like CAT enzymes, the utilization of SOD-like nanozymes in

534 colorimetric probes typically depends on the multifunctional enzyme properties of the nanozymes.

535 **4. The application of nanozyme based on the colorimetric biosensor for biotoxins detection**

536

4.1. Mycotoxins detection

538   Mycotoxins, as one of the most alarming food and feed contaminants, are carcinogenic and highly

539   toxic secondary metabolites produced by specific fungi, predominantly molds, which have the

540   potential to contaminate a broad spectrum of crops (including nuts, grains, and legumes) and this,

541   in turn, can be transferred to various food products. These naturally occurring toxins pose a

542   substantial risk to both human, with exposure capable of inducing numerous adverse effects such

543   as acute poisoning, chronic ailments, and potentially cancerous consequences. Mycotoxins are

544   typically prevalent in cereals, grains, nuts, spices, coffee, cocoa, dried fruits, and animal-sourced

545   products such as milk and meat. Prominent and extensively researched mycotoxins comprise

546   aflatoxins, ochratoxins, fumonisins, trichothecenes, and zearalenone [86, 87]. Therefore, the

547   implementation of effective and innovate mycotoxin analytical detection methods, and alongside

548   that, novel nanomaterials has become pivotal for safeguarding humans against health dangers and

549   risks. This section has been conducted to review the major mycotoxins, including aflatoxin B_1

550   (AFB1) and ochratoxin A (OTA), detection based on nanozymes.

551

4.1.1. Aflatoxin

553   Aflatoxins are hazardous secondary metabolites primarily synthesized by *Aspergillus fungi*. These

554   toxins reveal significant mutagenic, carcinogenic, and teratogenic potency in both human and

555   animal subjects. Corn, rice, peanuts, dried fruits, spices, and dairy products can be considered the

556   most important source of these toxins. Among different aflatoxins, AFB_1 introduced the most

Analytical Methods Accepted Manuscript

557 perilous member of the aflatoxin group, as a group 1 carcinogen, responsible for major of all

558 aflatoxins-associated feed and food contamination [88, 89]. In this regard, the maximum allowable

559 limits of AFB_1 in foodstuffs were set a 1.0–20 µg/kg. The field of biosensors based on various

560 nanozymes including single-atomic nanozymes [90], MOFs [55], and metal nanoparticles [19] is rapidly

561 evolving, with ongoing research focused on understanding their mechanisms of action and

562 increasing their catalytic efficiency. In favor of the application of metal nanoparticles as

563 nanozymes, two metal components demonstrate better peroxidase catalytic performance than

564 monometallic nanozymes. For example, Zhao et al. [91], reported a surface-enhanced Raman

565 scattering (SERS) sensor based on gold-mercury nanoparticles (Au@HgNPs) coupled with carbon

566 dots (CDs) for AFB_1 determination. In this study, the poor colloidal stability and low enzyme-like

567 activity of the AuNPs were distinctly improved by using Hg^{2+}. This modification could be

568 beneficial for the oxidase-mimicking activity of the AuNPs, attributing to Hg^{2+} reduced to the

569 metallic (Hg^0) forming Au@HgNPs. Under optimal conditions, the presence of the target inhibited

570 the aggregation of Au@HgNPs particles, through oxygen atoms in the carbonyl group, which

571 caused SERS intensity. In 2022, Lai et al. [92], focused on introducing a simple and rapid synthesis

572 method of nanozyme by simply mixing Cu(II) and $K_3[Fe(CN)_6]$ for presenting a copper

573 hexacyanoferrate nanoparticles (CHNPs) in terms of AFB_1 detection. Elaborately, in contrast to

574 the common nanozyme synthesis methods which rely on re-synthesized nanomaterials, the

575 nanozyme was designed in this biosensing platform without requiring the tedious process and

576 preparation of nanomaterials. Therefore, this biosensing approach can broaden our horizon about

577 another important factor in terms of the application nanozyme in detection, which is tedious

578 nanozyme preparation, by offering a simple, rapid, and accessible way to generate the nanozyme

579 on-demand. Interestingly, bimetal nanozymes demonstrate better catalytic efficacy compared to

28

580   their single-metal counterparts, owing to the synergistic interplay between the two metal varieties.

581   Most recently, Wu and co-workers [93], exploited mesoporous SiO_2/gold-platinum (Au-Pt), m-SAP,

582   in the structure of colorimetric biosensing device for AFB_1 detection. In this protocol, the

583   mesoporous of SiO_2 nanospheres were loaded with Au-Pt, enjoying high catalase like activity. In

584   the absence of the target, the complementary DNA conjugated m-SAP was captured by aptamer-

585   magnetic nanoparticles and facilitated the 3,3′,5,5′-tetramethylbenzidine (TMB)/H_2O_2 coloring

586   system. The detection limit of the developed colorimetric aptassay was 5 pg/mL, 600-fold lower

587   than that of traditional ELISA. In addition, during interference testing, AFB_1 could be

588   differentiated from six other interfering substances. In order to achieve more a reliable and highly

589   sensitive nanozyme based on two metal varieties, Jiang and colleagues [94], exploited the advantages

590   of bimetallic MoS_2/Au nanozyme, as a substrate for immobilization of aptamer, in developing of

591   sandwich-based colorimetric aptasensor of AFB_1 (Figure 4). In this work, the synergic effect

592   between MoS_2 and Au increased catalysis activity and stability. In detail, the low Michaelis

593   constant (Km) and the high maximum reaction rate (Vmax) of MoS_2/Au in comparison of single-

594   component MoS_2 or Au nanomaterials demonstrated that stronger binding affinity and superior

595   catalytic efficiency, respectively. Importantly, the specific structure, the flower-like MoS_2/Au

596   composite, introduced numerous surface-active sites through its unique multilayered and porous

597   structure which was considered an excellent immobilization substrate of aptamers. Furthermore,

598   the high surface area and porous structure of silica aerogel modified stainless-steel mesh

599   (SiO_2/SSM) could immobilization of the negatively charged aptamer2. Under normal

600   circumstances, the construction of sandwich aptassay was conducted by capturing AFB1 via

601   SiO_2/SSM, followed by binding of the MoS_2/Au/aptamer1. This structure was successfully

602 employed to quantify AFB$_1$ in different real food samples including peanut, corn, and wheat, with

603 negligible matrix effects (90.84%-106.11%) and recoveries of 88.52%-113.40%.

604
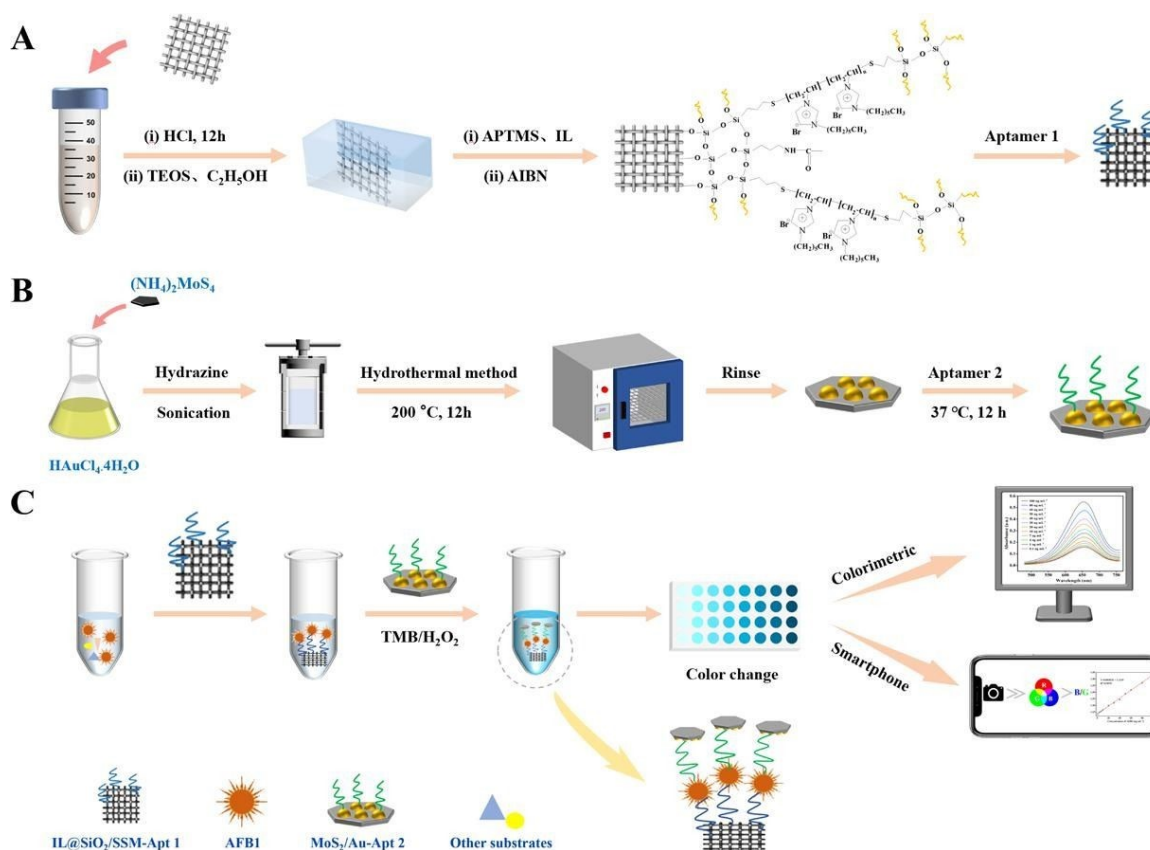
605 **Figure 4(A-C)**. Representation of colorimetric aptasensor based on MoS$_2$/Au for AFB$_1$

606 determination. Reproduced with permission from ref [94] Copyright Elsevier Science, 2024.

607 Another excellent example of this concept was implemented in colorimetric and photothermal

608 dual-mode immunoassay using peroxidase-like activity of Pt supported on nitrogen-doped carbon

609 for AFB$_1$ quantification [95]. As shown in Figure 5, the immune competition conducted between

610 glucose oxidase (GOx)-labeled AFB$_1$-bovine serum albumin (BSA) and AFB$_1$, therefore releasing

611 GOx to catalyze the glucose production of H$_2$O$_2$. Under normal condition, the colorimetric signal

612 was produced due to oxidization of TMB to TMBOx. Along with the colorimetric signal, a thermal

30

613   signal was achieved when TMBOx underwent photothermal conversion under 808 nm laser

614   irradiation. The fabricated biosensor was able to detect AFB_1 with a LOD of 0.22 and 0.76 pg/mL.

615
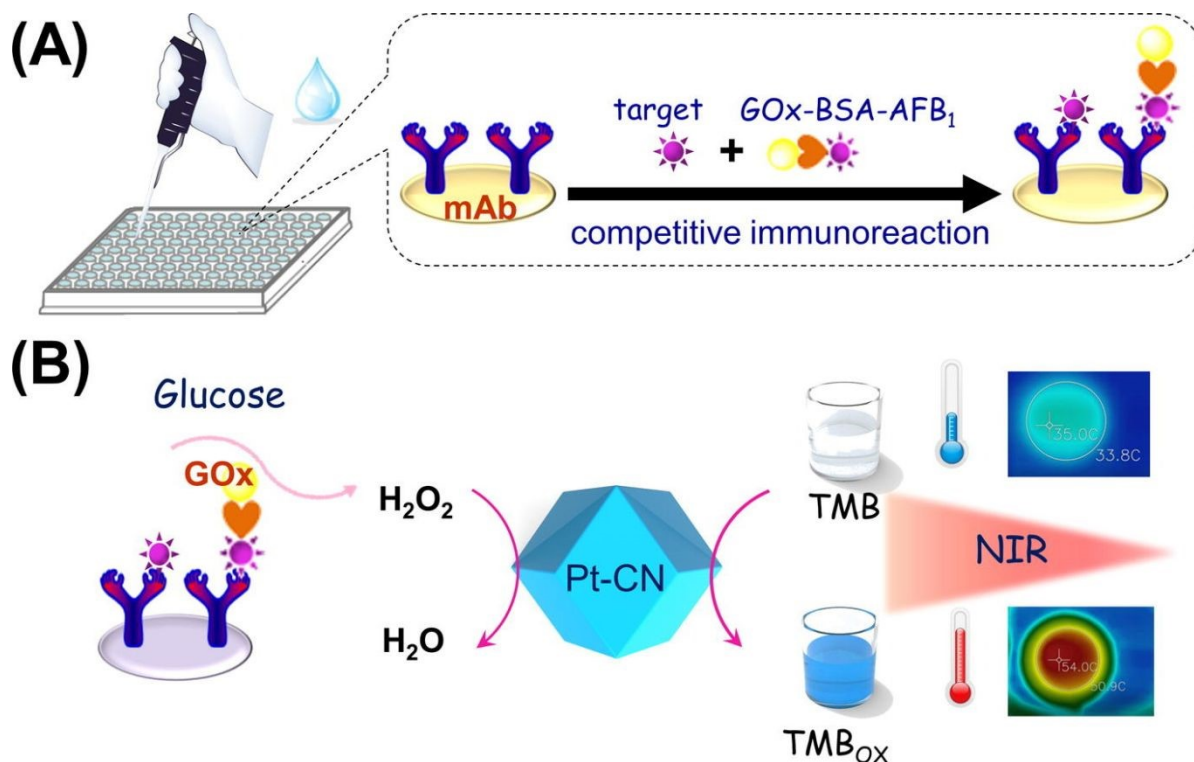
Figure 5. **(A)** Competitive-based immunosensor exploiting GOx-labeled AFB_1-BSA conjugate as

617   the tag. (B) Illustration colorimetric and photothermal measurement based on H_2O_2-responsive

618   peroxidase-like activity of Pt-CN. Reproduced with permission from ref [95]. Copyright Elsevier

619   Science, 2019.

620   The application of multimodal biosensors based on nanozyme in AFB_1 determination can

621   introduce different signals, extending the linear range of quantification. In addition, these signals

622   can verify each other to improve the accuracy of biosensing approaches [96, 97]. Another dual-mode

623   approach for AFB_1 quantification based on Ag@Au IP6 bifunctional nanozyme, with peroxidase-

624   like activity and SERS effect, was reported by Tan and colleagues [98]. For this purpose, the surface

625   of magnetic particles was decorated with AFB_1 aptamers along with a trigger probe. In the presence

626 of the target, the conjugation of targets with specific aptamers led to the trigger probe and this, in

627 turn, initiated a hybridization chain reaction (HCR) which introduced alkaline phosphatase (ALP),

628 catalyzing the self-assembly of the Ag@Au IP6 nanozyme. The constructed nanozyme revealed

629 increased peroxidase-like activity, improving the oxidation of TMB to the blue-colored TMBOx,

630 additionally, the core-shell structure of that also enabled strong SERS enhancement of the TMBOx

631 signal.

632 Particularly, in light of economic discussion, substituting precious metals, which contribute to

633 nanozymes, with more affordable transition metals, using in the structure of nanozymes can

634 markedly diminish the expenditure associated with nanozymes. For instance, Cai et al. [99], designed

635 a novel colorimetric nanozyme-based lateral flow assay (LFA) based on MnO_2 nanosheets (MnO_2

636 NSs) as an oxidase mimics and catalytic label for AFB1 determination. As shown in Figure 6A,

637 the test (T) line of the strip was decorated with anti-AFB_1 antibody-conjugated MnO_2 NSs for

638 capturing AFB_1. Attractively, thanks to the properties of MnO_2 NSs in catalyzing the oxidation of

639 TMB, TMB solution was added onto the T-line. When the target was added to the immunosensing

640 device, the oxidation could provide a visual color signal which was inversely proportional to the

641 AFB_1 concentration in the sample. The reported nanozyme-strip bioassay revealed a LOD of 15

642 pg/mL for AFB_1, over 100-fold lower than the maximum limit set by the European Union. On the

643 other hand, both of the instability of the colloidal nature of nanozymes and their complicated

644 interactions with bioreceptors can limit nanozyme exploitation in LFA. In this light, it is crucial to

645 rationally design nanozyme-based signal labels with features that facilitate easy functionalization,

646 good dispersibility, distinctly visible color, and enzymatic activity [100]. These features are pivotal

647 for increasing the applicability of nanozymes in LFA applications. A good example of this concept

648 was prepared in another transition metal, CuCo, which was coated by polydopamine (PDA) with

Analytical Methods Accepted Manuscript

649 excellent biocompatibility, good adhesion, and rich functional groups (chinone, imine, and amine),

650 leading to good hydrophilicity and binding ability with biomolecules [101]. In this protocol, the

651 carboxyl-functionalized aptamers were conjugated with CuCo@PDA nanozyme via amide

652 condensation reactions. The fabricated probe was used on the surface of the T line and the

653 difference of color with/without the presence of the target was the principle of detection (Figure

654 6B). Further, the ability of the nanozyme to catalyze the oxidation of TMB-H_2O_2 could amplify

655 the color change on the T-line. To illustrate, the visual LOD was reduced to 0.1 ng/mL by the

656 TMB-H_2O_2 catalytic amplification. In 2024, Fan and colleagues [102], designed another

657 functionalized nanozyme, flower-like L-cysteine-functionalized FeNi bimetallic nanoparticles (L-

658 Cys-FeNiNPs), with excellent peroxidase-like catalytic activity in colorimetric aptasensor for

659 detection of AFB_1. In the reported nanozyme, the peroxidase-like activity was attributed to the

660 generation of superoxide radicals ($\bullet O_2^-$) and holes (h^+) that were produced through the catalysis,

661 and alongside that, the high selectivity of probe was described as the conjugation of specific

662 aptamer with L-Cys-FeNiNPs via EDC/NHS chemistry and streptavidin-biotin interaction. Indeed,

663 like previous modification, the decoration of FeNiNPs with L-Cys not only can help increase the

664 dispersibility and stability of the FeNiNPs, but also the biocompatibility and functionalization

665 capability of nanozyme significantly improved. In the presence of the target, the reduction of the

666 active sites of the L-Cys-FeNiNPs suppressed the TMB oxidation and reduced the color signal.

Analytical Methods Accepted Manuscript
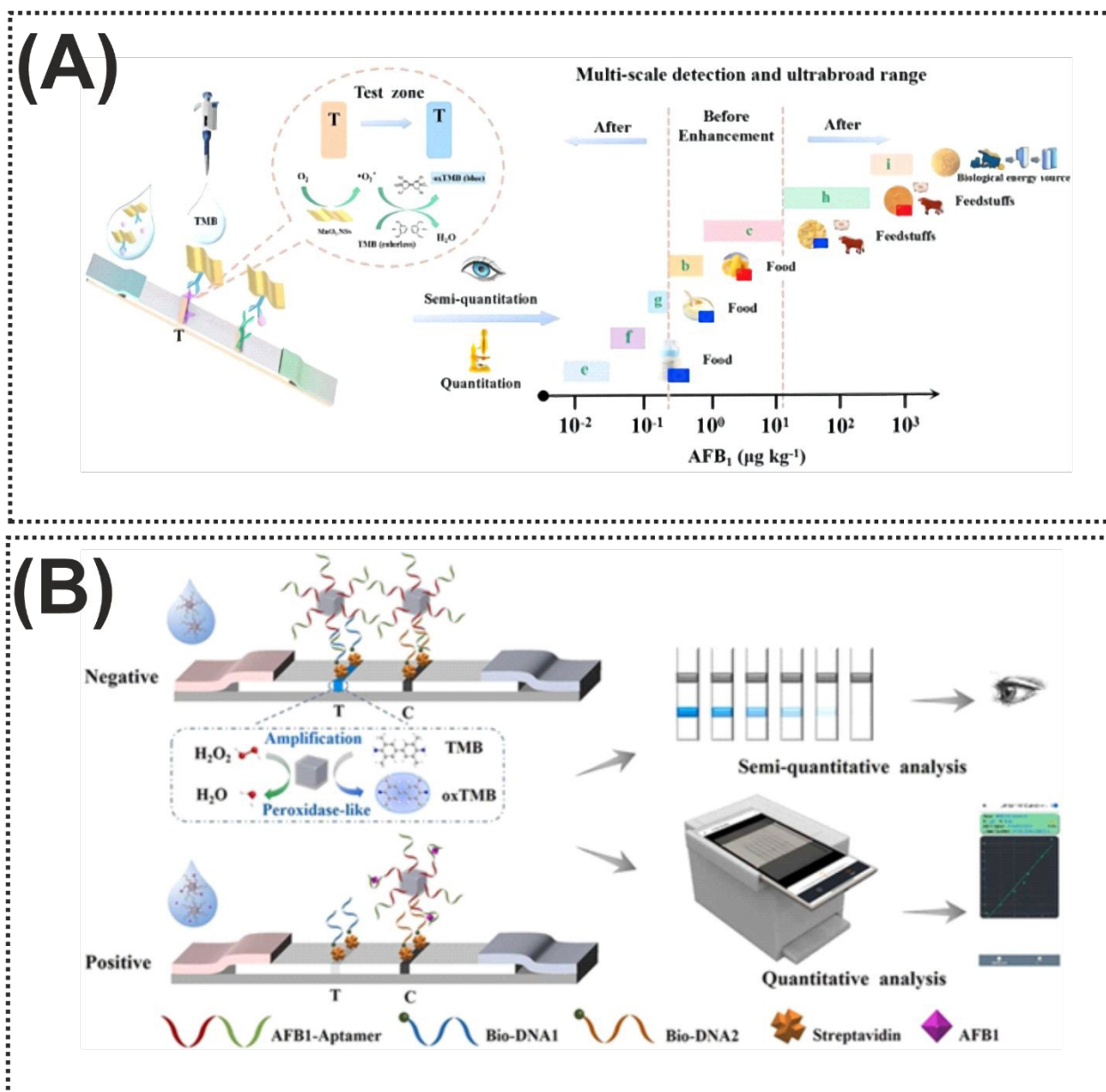
Figure 6A. Schematic of nanozyme-strip bioassay based on MnO_2 NSs for AFB_1 detection. Reproduced with permission from ref [99]. Copyright Elsevier Science, 2022. **Figure 6B.** Illustration of using CuCo@PDA in the structure of LFA for AFB_1 quantification. Reproduced with permission from ref [101]. Copyright Elsevier Science, 2024.

Along with metallic-based nanozymes, the application of metal-organic frameworks (MOFs) can be considered as a high potential nanozyme for quantification of AFB_1. Among different MOFs,

674   porphyrin (PCN)-based organic linkers were employed for self-assembly with metal nodes,

675   leading in the development of MOFs with different structures and functions. On the other hand,

676   accessing the active sites within MOFs remains challenging. One of the efficient solutions is based

677   on hybrid nanomaterials, which have been attributed to using platinum nanoparticles Pt NPs on

678   two-dimensional support substrates [103, 104]. As example, Zhang et al. [105], reported a novel

679   colorimetric approach exploiting Pt@PCN-222 nanozyme, with oxygen vacancies, for AFB_1

680   detection. The detection principle of this study was operated according to the oxidization of the

681   2,2′-azino-bis(3-ethylbenzthiazoline-6-sulfonic acid (ABTS) substrate to produce a blue-green

682   colored product. In the presence of the target, the binding of Pt@PCN-222 with the target caused

683   inhibition which decreased the number of active Pt@PCN-222 conjugates available for the ABTS

684   oxidation reaction. Another technique for addressing accessibility to the active sites of MOFs is

685   operated based on a synthesis technique, NanoMOFs, can accelerate substrate diffusion in catalytic

686   MOF material and this, in turn, provides greater external surface area and lower diffusion barriers.

687   For instance, Peng and co-workers [106], developed a sensitive, reproducible, and accurate

688   colorimetric immunoassay based on NanoPCN-223(Fe) with high peroxidase-like activity and

689   excellent dispersion for AFB1 determination (Figure 7). In detail, the implantation of NanoPCN-

690   223(Fe) in the structure of colorimetric technique which produced color by catalyzing the

691   oxidation of the colorless substrate TMB in the presence of H_2O_2. To illustrate, through the

692   catalyzing process, the nanozyme generated hydroxyl radicals (•OH), from H_2O_2, which oxidize

693   the TMB substrate, converting the colorless TMB to the blue ox-TMB. Under normal conditions,

694   the conjugation of the nanozyme and the target inhibited catalyzed oxidation of TMB which

695   reduced the intensity of color.

696 All things considered, the application of nanozymes based on metal nanoparticles and MOFs can

697 be considered efficient materials for aflatoxins detection. The investigation of these materials is

698 based on two metals varieties, bimetallic and affordable materials, and alongside that, the

699 amplification techniques can broaden our horizon about the performance of nanozymes in

700 colorimetric approaches for the detection of aflatoxins.
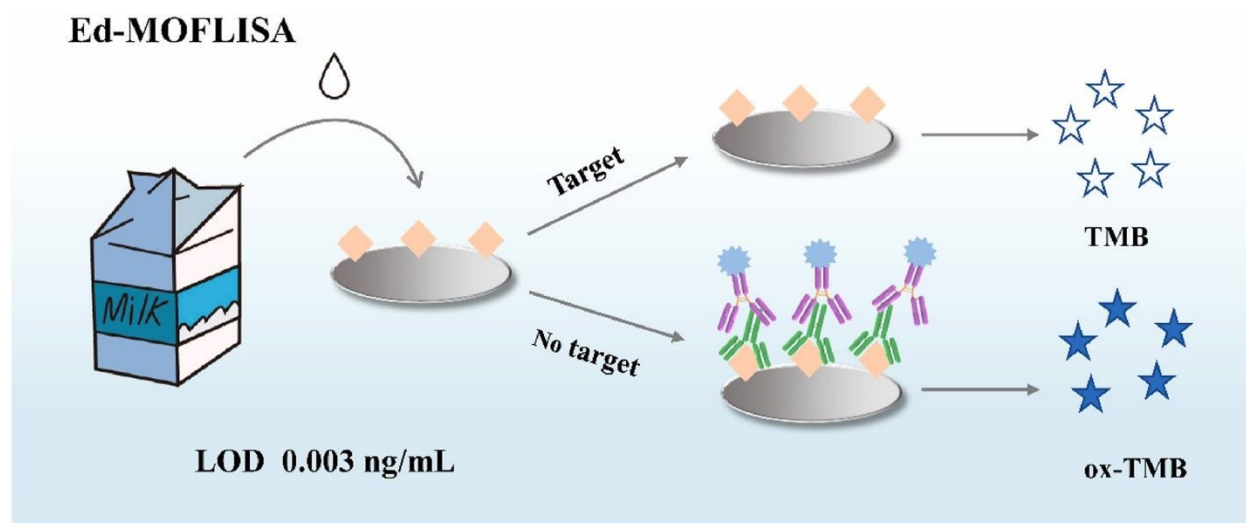
701

702 **Figure 7**. Illustration of the application of NanoMOFs for colorimetric detection of AFB_1.

703 Reproduced with permission from ref [106]. Copyright Elsevier Science, 2022.

704 **4.1.2. Ochratoxin A**

705 According to the International Agency for Research on Cancer, Ochratoxin A, as a possibly

706 carcinogenic to humans (Group 2B), is classified as one of the significant mycotoxins. To

707 elaborate, high chemical stability against heat treatments and hydrolysis through food processing

708 makes it one of the most dangerous poisons for human. This mycotoxin originates from the species

709 of fungi including *Penicillium verrucosum*, *Aspergillus carbonarius* , *Aspergillus ochraceus*, and

710 *Aspergillus niger* [107, 108]. Over the last decades, the advent of nanozyme has revolutionized multiple

711 domains in detection of OTA. Interestingly, the investigation of common structures of reported

Analytical Methods Accepted Manuscript

712 nanozymes can open new doors in terms of quantification of OTA. One of the common structures

713 is spinels which form huge families, and they consist of one or more metal elements. Among them,

714 spinel-type metal oxides, with the formula of AB_2O_4, enjoy superior promoting nanozyme

715 performance over other metal oxides due to controllable structure, composition, valence, and

716 morphology [109, 110], For example, Huang and co-workers [111], employed OTA-specific aptamer on

717 the surface of manganese cation substituted cobalt oxide ($MnCo_2O_4$) for OTA determination. As

718 shown in Figure 8, the attachment of aptamer on the surface of the nanozyme inhibited the

719 nanozyme activity of spinel $MnCo_2O_4$ through aptamer-target complex, presenting a new

720 colorimetric aptasensor. Under normal conditions, the developed aptassay could able to detect

721 OTA with a LOD of 0.08 ng/mL.

722
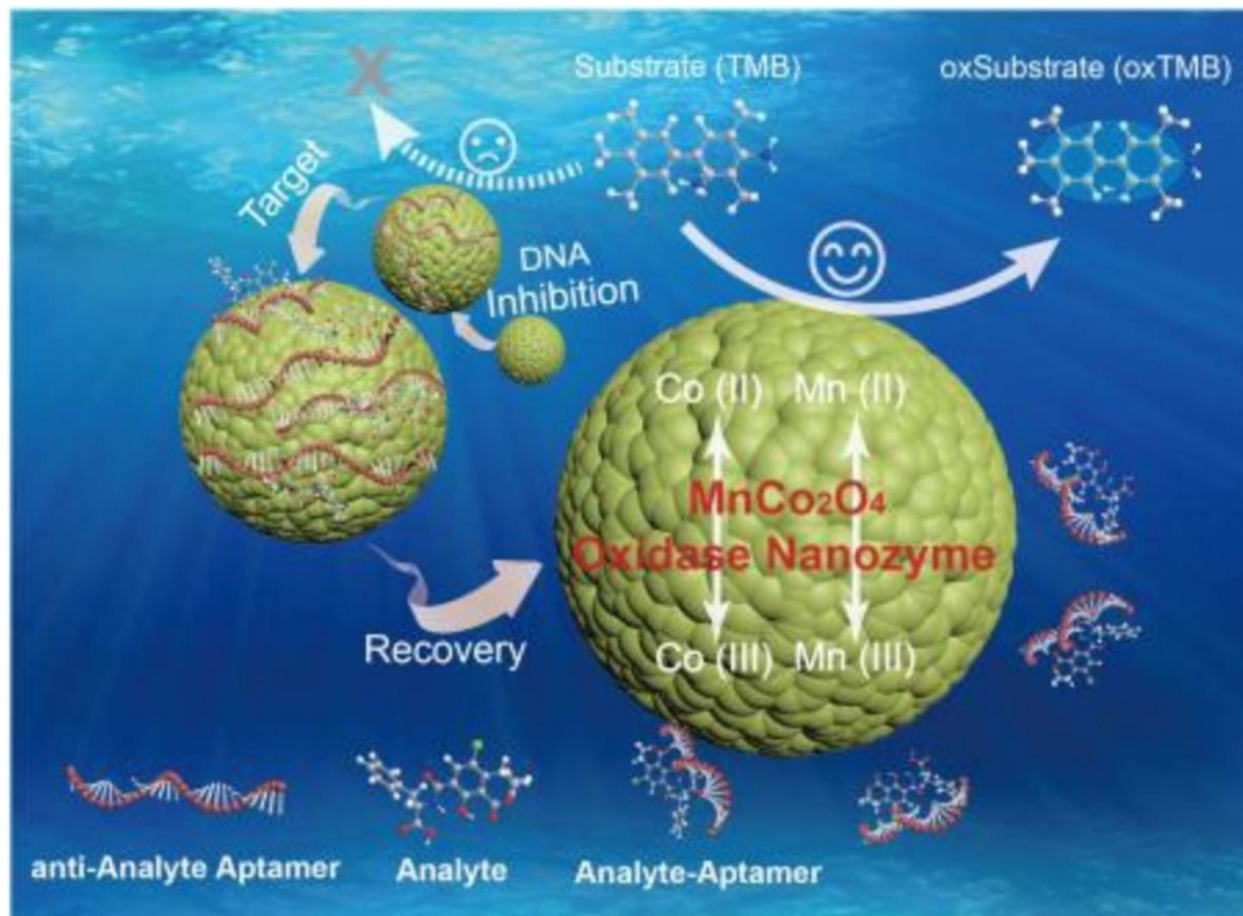
Figure 8. Schematic of using $MnCo_2O_4$ in the structure of colorimetric aptasensor for OTA

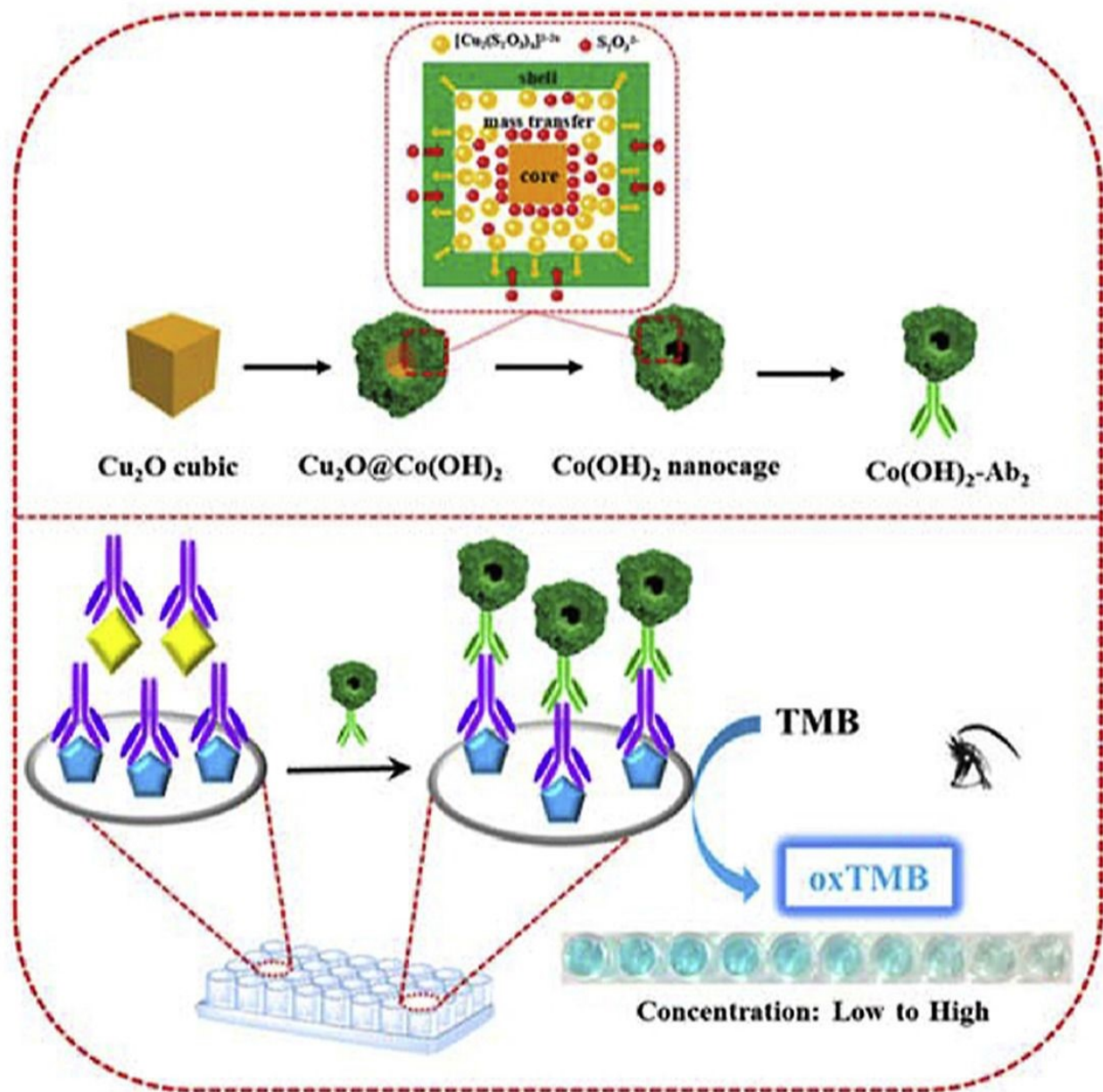determination. Reproduced with permission from ref [111]. Copyright Elsevier Science, 2018.

The distribution of cations among the octahedral and tetrahedral sites in the crystal structure can

introduce inverse spinel structure, with a formula of $B(AB)O_4$, which demonstrates different

electronic and magnetic features compared to the spinel structure [112]. Most recently, Liu and

colleagues [113], improved the performance of anti-spinel structure by using Au and Pt in the

structure of Fe_3O_4, through the ionic liquid (IL) as the cross-linker, for capturing synergistic

interaction between the alloy atoms. In this work, the surface of designed nanozyme was modified

with complementary DNA for conjugating with stainless steel mesh-aptamer. In the presence of

the OTA, the binding of the target with aptamer caused to separate signaling probe

($AuPt@IL@Fe_3O_4$) and this, in turn, was used in a tube containing a tube with H_2O_2 and TMB for

observe the color change. All in all, the inverse spinel and spinel structures introduce the effective

bioreceptor immobilization and high catalytic activity, increasing the performance of biosensors.

However, the limited surface area and non-optimal electronic properties of spinel structure can

restrict their application. In terms of inverse spinel, although magnetic features and high catalytic

activity improve their performance, a complex synthesis processes can limit their nanozyme-based

application.

Along with these structures, tetragonal crystals and nanocubes structures are other structures used

in the development of nanozyme for OTA detection. To illustrate, tetragonal crystal systems have

been widely exploited in biosensors based on nanozyme owing to several advantages such as high

surface area to volume ratio, stability, electronic features, high catalytic activity, and versatile

functionalization [114]. Currently, one of the excellent examples of using nanozyme-based tetragonal

crystal system for detection of OTA was developed by Tian and co-workers [115]. In this protocol,

746 the principle of this study was measuring the oxidase-mimicking activity of MnO_2 nanosheets. For

747 this purpose, the decoration specific aptamer on the surface of aptamer was exploited for capturing

748 OTA, leading to the production of the alkaline phosphatase-modified complementary DNA and

749 the cascade reaction is triggered by the product (ascorbic acid) of alkaline phosphatase catalysis.

750 The ascorbic acid reduced the oxidase-mimicking activity of MnO_2 nanosheets, leading to a pale

751 color of the enzyme catalytic substrate. Another structure is layer structure, with unique benefits,

752 which can provide efficient nanozymes in quantification of OTA. In 2020, Zhu et al. [116], fabricated

753 a novel colorimetric immunosensor based on cobalt hydroxide nanoparticle (Cu_2O) nanocubes,

754 with specific properties such as high surface area and high catalytic activity, for OTA

755 quantification (Figure 9). In detail, the decoration microwell plate with dopamine was modified

756 with OTA and ab_1 and, followed, $Co(OH)_2$-Ab_2 bounded to the prepared substrate. Under optimal

757 circumstances, the difference of the color changes of TMB from $Co(OH)_2$ nanocage in the absence

758 of H_2O_2 could present an efficient biosensing platform with a linear range and detection limit of

759 0.5 ng/L to 5 µg/L and 0.26 ng/L, respectively. Despite the high surface area and catalytic activity

760 of nanocubes structure, the stability issue in some conditions and aggregation of cubes be

761 considered important disadvantages of this structure. In addition, tetragonal crystal systems suffer

762 from limited surface area.

Analytical Methods Accepted Manuscript

763

Figure 9. Illustration of colorimetric immunoassay based on Cu_2O nanocubes for detection of

OTA. Reproduced with permission from ref [116]. Copyright Elsevier Science, 2020.

4.2. Marine toxins detection

Marine toxins, as poisonous substances, can be considered as natural metabolites which are

produced by numerous such as bacteria, algae, and many marine invertebrates. Among them, algal

toxins (including ciguatera toxin, domoic acid, and saxitoxin), invertebrate toxins, and some

770   bacterial toxins may concentrate on various organisms through the food web. The negative

771   consequences of these toxins in both humans and animals are undeniable [117, 118]. Importantly,

772   various bioreceptors/receptors can improve the performance of nanozyme-based colorimetric

773   biosensors for determination of marine toxins. Antibodies, as one of the important bioreceptors,

774   have been used in antibody-antigen interaction for presenting sensitivity and specificity detection

775   approaches of marine toxins. Interestingly, the integration of nanozyme in the structure of

776   colorimetric immunosensors can improve analytical signal owing to the catalyzation of enzymatic

777   reaction by nanozyme, which increases the color intensity. For example, Hendrickson and co-

778   workers [119], conjugated Au@Pt nanozyme with an antibody for enhancing label of okadaic acid

779   quantification. The tendency of Au@Pt nanozyme to conjugate with anti-mouse antibodies, rather

780   than anti-okadaic acid antibodies, could provide an excellent situation for an indirect competitive

781   immunoassay format. This phenomenon led to unproductive immune binding without signal

782   change is excluded, resulting in improving sensitivity of immunoassay. When the target was added

783   to the system, the okadaic acid competed with the okadaic acid on conjugate pad for binding with

784   anti-okadaic acid antibodies and were immobilized on the T line of LFA.

785   The lack of chemical and thermal stability of antibodies, in harsh environmental circumnutates,

786   can make them sensitive to degradation and denaturation. Furthermore, the high cost of production

787   and purification of these bioreceptors can be considered another significant issue. In this regard,

788   competitive colorimetric was implanted in aptasensors based on AuNPs nanozyme for sensitive

789   and selective quantification of saxitoxin [120]. In this study, the competition of saxitoxin in samples

790   with immobilization saxitoxin was a principle of the developed aptassay. To illustrate, in the

791   presence of the target, the separation of specific aptamer from magnetic particles was conducted

792   and this, in turn, led to triggering the hybridization chain reaction. The colorimetric signal was

793 improved by amplifying catalytic activity of the AuNPs nanozymes. Similarly, in many

794 colorimetric aptasensor studies, the adsorption of aptamer could promote the enzyme-like activity

795 of AuNPs for saxitoxin determination [121, 122]. Elaborately, this phenomenon could enhance surface

796 negativity of nanozymes which increased adsorption and diffusion of positively charged substrates

797 of TMB, improving of catalytic efficiency. In 2022, Li and colleagues [123], reported a novel

798 aptasensor exploiting AuNPs@Fe^{2+} for multiple diarrheic shellfish poisons detection (Figure 10).

799 Indeed, the performance of nanozyme, in terms of chemical stability and peroxidase-like activity,

800 was improved by using Fe^{2+} in the structure of AuNPs. Furthermore, the high affinity of terminal-

801 fixed aptamer (TF-DSP) was used in this study for the simultaneous detection of three diarrheic

802 shellfish poisons. Under normal circumstances, the catalyze of TMB/H_2O_2/acetic acid due to the

803 excellent peroxidase-like activity and the brilliant selectivity of aptamer could introduce a

804 biosensing platform with a linear range and LOD of 0.4688–7.5 nM and 86.28 pM, respectively.

805
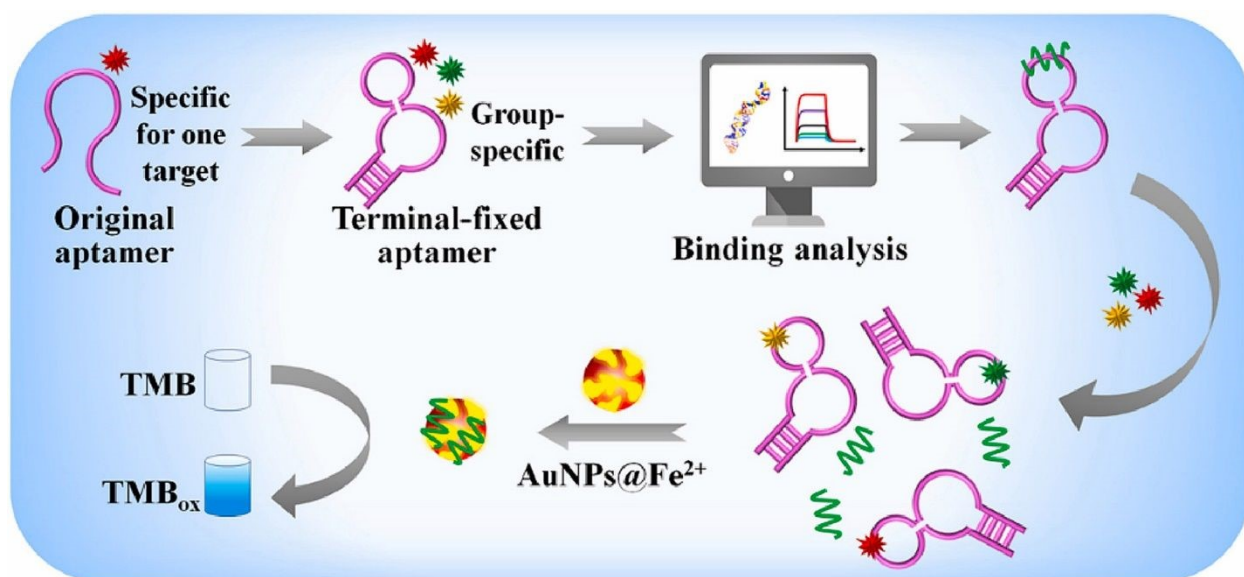
806 **Figure 10**. Schematic of colorimetric aptassay using decoration AuNPs with Fe^{+2} for multiple

807 diarrheic shellfish poisons detection. Reproduced with permission from ref [123]. Copyright Elsevier

808 Science, 2022.

809 The complex immobilization process on the surface of nanozyme and the side effect of potential

810 interferences, in real samples, can considered the most important limitation of using aptamers in

811 the nanozyme structure. In addition, in terms of overcoming stability issues of combination of

812 antibodies with nanozyme, molecularly imprinted polymer (MIP), as artificial antibody and

813 antigen systems, attracted considerable attention for marine toxins detection [124, 125]. Most recently,

814 Wu et al. [126], integrated a MIP with Au-Pt nanoparticles modified Fe_3O_4 magnetic nanozymes for

815 introducing an efficient biosensor of saxitoxin. For this purpose, Au-Pt nanoparticles were loaded

816 in Fe_3O_4 magnetic and, subsequently, thanks to the hydrolysis polymerization reaction, the

817 decoration modified Fe_3O_4 magnetic nanozymes with MIPs were prepared. In the presence of the

818 target, catalyzed the oxidation of TMB enabled the developed biosensing approach for detection

819 saxitoxin with a detection limit of 3.1 nM. Potential interference in signal transduction, durability,

820 and stability issues can be supposed most important limitation of MIPs. In order to address these

821 limitations, scholars must pay special attention to the fabrication optimized and compatible MIP-

822 nanozyme platforms. For instance, Cho and colleagues [127], used peptide (as both the imprinting

823 template and the signal peptide), instead of antigen or aptamer, for designing competitive

824 colorimetric quantification of saxitoxin. In this light, the exploitation of specific peptides of

825 saxitoxin could overcome difficulty of aptamers and antibodies removal in biosensors based on

826 MIP-nanozyme. In addition, the integration MIP with specific peptide of saxitoxin was measured

827 with $AuNP/Co_3O_4@Mg/Al$. In the presence of the target, the less specific peptide of saxitoxin was

828 conjugated with MIP, leading to intensity of color change.

4.3. Bacterial food toxins

829

830 Nowadays, bacteria food toxin, which is macromolecule mainly of protein origin, is one the main

831 issues in the realm of food safety. These microorganisms can produce toxins in food or once the

832   pathogen has colonized the digestive tract. These types of toxins damage in a specific organ of the

833   host. To illustrate, such toxins cause foodborne diseases including vomiting, nausea, abdominal

834   cramps, and diarrhea. [128, 129]. Despite the fact that the field of research about detection bacterial

835   toxins is very wide, researchers attempted to use different nanomaterials in the structure of

836   nanozymes for amplification of detection signal. Various forms of Au-based nanomaterials such

837   as AuNPs gold nanostars (AuNSs) have been exploited as one of the important nanomaterials to

838   amplify the signal due to several benefits such as excellent stability, repeatability, and accuracy.

839   These nanomaterials gained great attention due to their ability to couple and integrate with different

840   bioreceptors and nanomaterials for acting as a nanozyme through chemical bonds and electrostatic

841   adsorption. As for labelling nanomaterials, Ren et al. [130], used the seed growth method for

842   assembling AuNSs in the structure of Mn/Fe-MIL(53) for introducing an efficient nanozyme in

843   colorimetric and SERS detection of Shiga toxin type II. As shown in Figure 11A, in terms of

844   construction signal probe which could oxidize colorless TMB into blue color oxTMB, the surface

845   of Mn/Fe-MIL(53) was decorated with AuNSs for providing an excellent for immobilization of

846   SH-complementary DNA, through Au–S bonding. In addition, in favor of capturing probe,

847   streptavidin-labeled magnetic beads were modified with a specific biotin-labeled aptamer. In the

848   presence of the target, the conjugation of aptamer with target the release of signal probes from the

849   complex and bring an enhancement of SERS and colorimetric signals. In the reported dual-mode,

850   the integration of SERS and colorimetric approaches introduced complementary and validated

851   results, improving the reliability of the Shiga toxin type II detection. In another example of Au-

852   based nanozymes, Liang and co-workers [131], designed a novel dual-signal probe (AuPt

853   nanoparticle-loaded single atom nanocomposite, AuPt@Fe-N-C) for *Staphylococcus aureus*

854   enterotoxin B quantification (Figure 11B). For this purpose, the ab_1 was immobilized on the

855 surface of AuPt@Fe-N-C and this was used for sandwich structure. In addition to the target to the

856 system, the ab_1-*Staphylococcus aureus* enterotoxin B-ab_2 was performed in a 96-well plate which

857 could oxidation TMB from colorless to blue with a detection limit of 0.066 7 pg/mL. Along with

858 Au-based nanozyme, the unique properties and structure of rhodium (Rh), a non-toxic transition

859 metal, was exploited for staphylococcal enterotoxin B determination in milk samples [132]. The

860 implementation of Rh, with peroxidase-like catalytic activity, on the sensing zone of LFA could

861 able to detect staphylococcal enterotoxin B with a detection limit of as low as 1.2 pg/mL.

Analytical Methods Accepted Manuscript

862

46
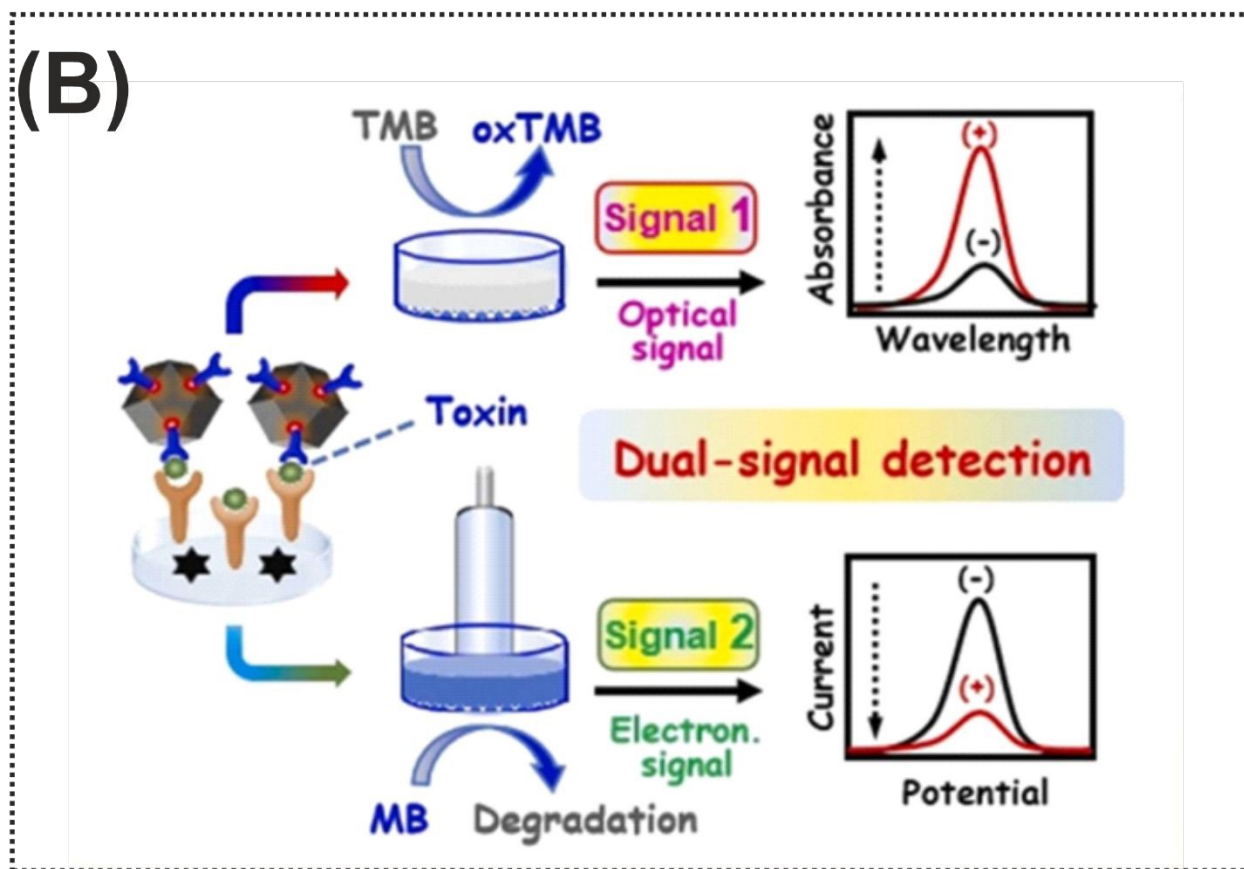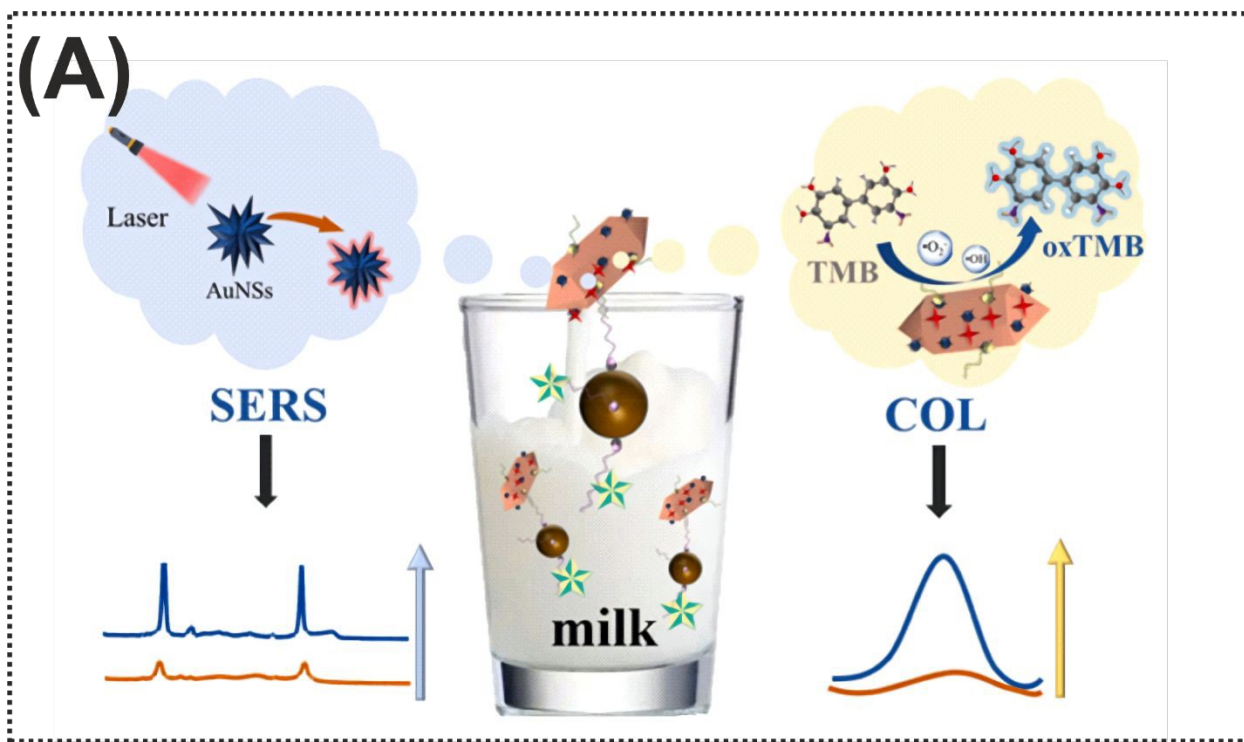
863 **Figure 11. (A)** Representation of dual-mode colorimetric and SERS biosensor based on Mn/Fe-

864 MIL(53)@AuNSs for Shiga toxin type II detection. Reproduced with permission from ref [130] (B)

865 Illustration of dual-signal electrochemical and colorimetric detection of *Staphylococcus aureus*

866 enterotoxin B [131] . Copyright Elsevier Science, 2024.

867 **5. Theranostic applications of nanozymes for biotoxins**

868 Nanozymes catalytic theranostics introduces an innovative and novel strategy for theranostic

869 platforms, integrating detection and treatment in a single system [133]. The importance of these

870 platforms is highlighted in preventing the spread of biotoxins in contamination outbreaks by

871 intervention to neutralize biotoxins and monitoring them [134]. In favor of the detection of biotoxins,

872 catalytic color changing reaction conducts for achieving sensitive colorimetric sensors. In terms

873 of naturalization and degradation of biotoxins, the oxidation and hydrolysis of biotoxins break

874 these toxins by-products chemical down into non-toxic components by using nanozymes is an

875 efficient strategy for rendering them harmless [135, 136]. Numerous techniques were exploited for

876 biotoxins degradation such as UV method for marine biotoxins, demonstrating resistance to

877 photodegradation, On the other hand, high performance degradation with $UV/S_2O_8^{2-}$ and

878 UV/H_2O_2 was achieved [137, 138]. In addition, biodegrading ATX-a into a nontoxic byproduct by

879 *Bacillus* strains such as *Bacillus flexus* SSZ01 and *Bacillus* strain AMRI-03 can supposed high

880 performance method for water treatment like rapid degradation of saxitoxins, which is directly and

881 indirectly associated with food safety [139]. Furthermore, MOF-derived nanozymes was used as a

882 high potential materials in the neutralization process [140]. Future research should be focused on the

883 theranostic application of nanozymes for biotoxins due to a lack of research studies in this field.

884 In other words, this field can advance biosensors and detoxification systems, managing biotoxin

885 threats in different environments and food matrices.

886   **Table 1.** Comparison reported of colorimetric sensors with nanozymes for detection of different
887   biotoxins.

Nanozymes	Enzyme activity	Substrate	Target	Linear range	LOD	Ref.
Au@HgNPs	OXD	TMB	AFB_1	0.125 to 87.5 µg/L	0.08 µg/L	[91]
CHNPs	OXD	TMB	AFB_1	1 pg/mL to 20 ng/mL	0.73 pg/mL	[92]
Au-Pt	OXD	TMB	AFB_1	0.1 to 500 ng/mL	5 pg/mL	[93]
MoS_2/Au	POD	TMB	AFB_1	1 to 100 ng/mL	0.25 ng/mL	[141]
Pt-CN	POD	TMB	AFB_1	1.0 pg/mL to 10 ng/mL	0.22 pg/mL	[95]
Ag@Au IP6	POD	TMB	AFB_1	2 pg/L to 200 pg/L	0.58 pg/L	[98]
MnO_2 NSs	OXD	TMB	AFB_1	0.01 to 150 ng/mL	0.015 ng/mL	[99]
CuCo@PDA	POD	TMB	AFB_1	0.01 to 50 ng/mL	2.2 pg/mL	[101]
FeNiNPs	POD	TMB	AFB_1	0.12 to 2 µg/mL	36.57 ng/mL	[102]
Pt@PCN-222	OXD	ABTS	AFB_1	0.1 to 10 ng/mL	0.074 µg/L	[142]
NanoPCN-223	POD	TMB	AFB_1	0.05 to 10 ng/mL	0.003 ng/mL	[106]
$MnCo_2O_4$	OXD	TMB	OTA	0.1 to 10 ng/mL	0.08 ng/mL	[111]
Fe_3O_4	POD	TMB	OTA	5 to 100 ng/mL	0.078 ng/mL	[113]
MnO_2 NSs	OXD	TMB	OTA	1.25 to 250 nM	0.069 nM	[115]
Cu_2O nanocubes	OXD	TMB	OTA	0.5 ng/L to 5 mg/L	0.26 ng/L	[116]
Au@Pt	POD	TMB	Okadaic acid	0.8 to 6.8 ng/L	0.5 ng/L	[119]
AuNPs	POD	TMB	Saxitoxin	78.13 to 2500 pM	42.46 pM	[120]
AuNPs@Fe^{2+}	POD	TMB	Okadaic acid, dinophysistoxin-1, and dinophysistoxin-2	4688 to 7.5 nM	86.28 pM	[123]
Fe_3O_4@Au-Pt	OXD	TMB	Saxitoxin	0.01 to 100 µM	3.1 nM	[126]
AuNP/Co_3O_4@Mg/Al cLDH	POD	TMB	Saxitoxin	0 to1000 ng/mL	3.17 ng/mL	[127]
Mn/Fe-MIL(53)@AuNSs	POD	TMB	Shiga toxin type II	0.05 to 500 ng/mL	26 pg/mL	[130]
AuPt@Fe-N-C	POD	TMB	*Staphylococcus aureus* enterotoxin B	0.0002 to 10.000 ng/mL	0667 pg/mL	[131]
Rh	POD	TMB	Staphylococcal enterotoxin B	0 to 2 ng/mL	1.2 pg/mL	[132]

888

Analytical Methods Accepted Manuscript

6. Conclusions and future perspectives

889

890 Numerous attempts have been undertaken to control biotoxins; however, their contamination

891 remains largely inevitable. Therefore, there is an urgent need for research to explore the biosensors

892 for the rapid, sensitive, and convenient detection of biotoxins, given the detrimental impact of

893 biotoxins on human health and food safety. So, as described in this literature update, owing to their

894 favorable catalytic activity, excellent stability, and low cost, nanozymes and nanozyme-based

895 biosensors have been extensively exploited to identify different biotoxins in food and

896 environmental samples. In particular, the combination of colorimetric biosensors and nanozymes

897 to construct an innovative biosensing scaffold provides a promising outlook in convenient,

898 sensitive, and rapid quantification of various biotoxins. Herein, we discuss the production,

899 characteristics, and application of nanozymes in colorimetric biosensors, focusing on their diverse

900 catalytic activities. Furthermore, a comprehensive overview of the research conducted on the

901 utilization of nanozyme-based colorimetric biosensors for the identification of biotoxins is

902 provided. Through deliberating the sensing approaches employed by nanozyme-based colorimetric

903 biosensors, it becomes evident that these biosensors serve crucial roles in the rapid diagnosis of

904 biotoxins. Besides, we highlight the recent advancements in portable technologies, including

905 hydrogels and paper-based platforms, that can be integrated with smartphones to enable on-site

906 detection. Although nanozyme-based colorimetric biosensors possess the features of fast response,

907 simple operation, high sensitivity, and low cost, they still have some challenges in several aspects.

908 i) Due to the inferior catalytic efficiency of nanozymes in comparison with natural enzymes, the

909 application of nanozymes with multiple catalytic and high activity can be considered one of the

910 efficient strategies. Indeed, multiple catalytic including peroxidase-like, oxidase-like, and

911 catalase-like activities can improve the performance of nanozymes. Furthermore, the concept of

912 high activate nanozymes is achieved by integration of nanozymes with different nanomaterials. As

913 well, the lower selectivity of nanozymes towards targets restricts specific recognition in the

914 detection process. Consequently, the development of novel nanozymes with enhanced specificity

915 could involve the integration of biomimetic recognition elements, such as MIPs, and exploring

916 additional technical approaches holds promise for future advancements in this area.

917 ii) Currently, an increasing number of studies are focusing on nanozymes exhibiting multiple

918 enzyme activities. However, the utilization of nanozymes with multiple enzyme performances in

919 colorimetric biosensors predominantly depends on their POD and OXD-like activities. Regulating

920 the predominant activity of nanozymes with multiple enzyme-like functions simultaneously poses

921 a significant challenge. This task necessitates a more precise comprehension of the catalytic

922 mechanisms underlying various enzyme activities, along with a thorough understanding of the

923 primary factors influencing these activities.

924 iii) The catalytic reactions occur in the specific regions on the nanozyme's surface which are

925 considered as active places. Generally, these active places are similarly operated based on the

926 active sites in natural enzymes. However, their function and structure can differ owing to the basic

927 differences between biological macromolecules and nanomaterials [143]. Elaborately, the presence

928 of a small number of amino acids can able natural enzymes to directly interact with the substrate.

929 Hydrophobic interactions and hydrogen bonding are the most important of these interactions,

930 providing the high efficiency and specificity substrate. On the other hand, specific atoms or

931 clusters of atoms on the surface of nanozymes act as active places. In detail, specific functional

932 groups or metal ions can mimic the catalytic functions of natural enzymes. In addition, the

933 chemical composition, size, and shape of nanozymes can impact on their catalytic activity [144].

934

935   To sum up, the investigation of nanozymes and nanozyme-based colorimetric represents merely

936   the initial phase of a vast field of study. Nevertheless, it is evident that these biosensors exhibit

937   significant promise in applications and merit further investigation. As research on progresses and

938   nanozyme-based colorimetric biosensors continue to evolve, it is anticipated that more cutting-

939   edge technologies and portable devices will be developed and extensively employed to safeguard

940   food and environmental integrity.

944   **References**

945   1.   M. Mahmoudpour, J. Ezzati Nazhad Dolatabadi, M. Torbati, A. Pirpour Tazehkand, A.
946   Homayouni-Rad and M. de la Guardia, *Biosensors and Bioelectronics*, 2019, **143**, 111603.
947   2.   M. Mahmoudpour, J. Ezzati Nazhad Dolatabadi, M. Torbati and A. Homayouni-Rad, *Biosensors*
948   *and Bioelectronics*, 2019, **127**, 72-84.
949   3.   J. Nicolas, R. L. Hoogenboom, P. J. Hendriksen, M. Bodero, T. F. Bovee, I. M. Rietjens and A.
950   Gerssen, *Global Food Security*, 2017, **15**, 11-21.
951   4.   M.-L. Liu, X.-M. Liang, M.-Y. Jin, H.-W. Huang, L. Luo, H. Wang, X. Shen and Z.-L. Xu, *Journal of*
952   *Agricultural and Food Chemistry*, 2024.
953   5.   F. Javaheri-Ghezeldizaj, M. Mahmoudpour, R. Yekta and J. Ezzati Nazhad Dolatabadi, *Journal of*
954   *Molecular Liquids*, 2020, **310**, 113259.
955   6.   C. Lin, Z.-S. Liu, C.-Y. Tan, Y.-P. Guo, L. Li, H.-L. Ren, Y.-S. Li, P. Hu, S. Gong and Y. Zhou,
956   *Environmental Science and Pollution Research*, 2015, **22**, 1545-1553.
957   7.   D. Liu, in *Molecular Medical Microbiology*, Elsevier, 2024, pp. 933-944.
958   8.   P. Sadeghi, H. Sohrabi, M. R. Majidi, A. Eftekhari, F. Zargari, M. de la Guardia and A. A.
959   Mokhtarzadeh, *TrAC Trends in Analytical Chemistry*, 2024, 117722.
960   9.   Y. Liu and F. Wu, *Environmental health perspectives*, 2010, **118**, 818-824.
961   10.   S. Siva, J.-O. Jin, I. Choi and M. Kim, *Biosensors and Bioelectronics*, 2023, **219**, 114845.
962   11.   M. Mahmoudpour, S. Ding, Z. Lyu, G. Ebrahimi, D. Du, J. Ezzati Nazhad Dolatabadi, M. Torbati
963   and Y. Lin, *Nano Today*, 2021, **39**, 101177.
964   12.   Z. Karimzadeh, M. Mahmoudpour, E. Rahimpour and A. Jouyban, *Advances in Colloid and*
965   *Interface Science*, 2022, **305**, 102705.
966   13.   T. A. Rocha-Santos, *TrAC Trends in Analytical Chemistry*, 2014, **62**, 28-36.
967   14.   Z. Golsanamlou, M. Mahmoudpour, J. Soleymani and A. Jouyban, *Critical Reviews in Analytical*
968   *Chemistry*, 2023, **53**, 1116-1131.
969   15.   Z. Khoshbin, M. Moeenfard, K. Abnous and S. M. Taghdisi, *Food Chemistry*, 2024, **433**, 137355.

Analytical Methods Accepted Manuscript

970   16.   L. Lu, R. Yu and L. Zhang, *Food Chemistry*, 2023, **421**, 136205.
971   17.   R. L. F. Melo, F. S. Neto, D. N. Dari, B. C. C. Fernandes, T. M. Freire, P. B. A. Fechine, J. M. Soares
972   and J. C. S. Dos Santos, *International Journal of Biological Macromolecules*, 2024, 130817.
973   18.   T. Vyas, V. Singh, P. Kodgire and A. Joshi, *Critical Reviews in Biotechnology*, 2023, **43**, 521-539.
974   19.   J. Qin, N. Guo, J. Yang and J. Wei, *Food Chemistry*, 2024, 139019.
975   20.   A. Baranwal, R. Shukla and V. Bansal, *TrAC Trends in Analytical Chemistry*, 2024, 117573.
976   21.   L. Yang, X. Xu, Y. Song, J. Huang and H. Xu, *Chemical Engineering Journal*, 2024, **487**, 150612.
977   22.   Z. Chi, Q. Wang and J. Gu, *Analyst*, 2023, **148**, 487-506.
978   23.   B. Unnikrishnan, C.-W. Lien, H.-W. Chu and C.-C. Huang, *Journal of Hazardous Materials*, 2021,
979   **401**, 123397.
980   24.   Y. Huang, J. Ren and X. Qu, *Chemical reviews*, 2019, **119**, 4357-4412.
981   25.   H. Wei, L. Gao, K. Fan, J. Liu, J. He, X. Qu, S. Dong, E. Wang and X. Yan, *Nano Today*, 2021, **40**,
982   101269.
983   26.   L. Zhang, H. Wang and X. Qu, *Advanced Materials*, 2024, **36**, 2211147.
984   27.   Z. Li, W. Liu, P. Ni, C. Zhang, B. Wang, G. Duan, C. Chen, Y. Jiang and Y. Lu, *Chemical Engineering
985   Journal*, 2022, **428**, 131396.
986   28.   Z. Lou, S. Zhao, Q. Wang and H. Wei, *Analytical chemistry*, 2019, **91**, 15267-15274.
987   29.   K. Fan, J. Xi, L. Fan, P. Wang, C. Zhu, Y. Tang, X. Xu, M. Liang, B. Jiang and X. Yan, *Nature
988   Communications*, 2018, **9**, 1440.
989   30.   P. Zhang, D. Sun, A. Cho, S. Weon, S. Lee, J. Lee, J. W. Han, D.-P. Kim and W. Choi, *Nature
990   communications*, 2019, **10**, 940.
991   31.   S. Pandit and M. De, *Nanoscale Advances*, 2021, **3**, 5102-5110.
992   32.   H. Sun, A. Zhao, N. Gao, K. Li, J. Ren and X. Qu, *Angewandte Chemie International Edition*, 2015,
993   **54**, 7176-7180.
994   33.   M. Mahmoudpour, J. E. N. Dolatabadi, M. Hasanzadeh, A. H. Rad, M. Torbati and F. Seidi, *RSC
995   advances*, 2022, **12**, 29602-29612.
996   34.   M. S. Kim, S. Cho, S. H. Joo, J. Lee, S. K. Kwak, M. I. Kim and J. Lee, *ACS nano*, 2019, **13**, 4312-
997   4321.
998   35.   Z. Wang, Z. Xu, X. Xu, J. Xi, J. Han, L. Fan and R. Guo, *Colloids and Surfaces B: Biointerfaces*, 2022,
999   **217**, 112671.
1000   36.   F. Li, J. Jiang, H. Peng, C. Li, B. Li and J. He, *Sensors and Actuators B: Chemical*, 2022, **369**,
1001   132334.
1002   37.   L. Zhu, W. Zeng, Y. Li, Y. Han, J. Wei and L. Wu, *Science of The Total Environment*, 2024, **921**,
1003   171236.
1004   38.   X. Liang, X. Wang, Y. Zhang, B. Huang and L. Han, *Journal of Agricultural and Food Chemistry*,
1005   2022, **70**, 3898-3906.
1006   39.   X. Zhang, Y. Xu, X. Wang, T. Chen, Q. Yao, S. Chang, X. Guo, X. Liu, H. Wu and Y. Cui, *Food
1007   Chemistry*, 2024, 140710.
1008   40.   C. Lu, L. Tang, F. Gao, Y. Li, J. Liu and J. Zheng, *Biosensors and Bioelectronics*, 2021, **187**, 113327.
1009   41.   S. Naveen Prasad, P. Weerathunge, M. N. Karim, S. Anderson, S. Hashmi, P. D. Mariathomas, V.
1010   Bansal and R. Ramanathan, *Analytical and Bioanalytical Chemistry*, 2021, **413**, 1279-1291.
1011   42.   D. Li, D. Dai, G. Xiong, S. Lan and C. Zhang, *Small*, 2023, **19**, 2205870.
1012   43.   P. T. Nguyen, J. Lee, A. Cho, M. S. Kim, D. Choi, J. W. Han, M. I. Kim and J. Lee, *Advanced
1013   Functional Materials*, 2022, **32**, 2112428.
1014   44.   Y. Lin, C. Xu, J. Ren and X. Qu, *Angewandte Chemie (International ed. in English)*, 2012, **51**,
1015   12579-12583.
1016   45.   L. Gao, J. Zhuang, L. Nie, J. Zhang, Y. Zhang, N. Gu, T. Wang, J. Feng, D. Yang and S. Perrett,
1017   *Nature nanotechnology*, 2007, **2**, 577-583.

Analytical Methods Accepted Manuscript

1018   46.   R. André, F. Natálio, M. Humanes, J. Leppin, K. Heinze, R. Wever, H. C. Schröder, W. E. Müller
1019   and W. Tremel, *Advanced Functional Materials*, 2011, **21**, 501-509.
1020   47.   A. B. Ganganboina and R.-a. Doong, *Sensors and Actuators B: Chemical*, 2018, **273**, 1179-1186.
1021   48.   H. Li, S. Zhao, Z. Wang and F. Li, *Small*, 2023, **19**, 2206465.
1022   49.   L. Han, H. Zhang, D. Chen and F. Li, *Advanced Functional Materials*, 2018, **28**, 1800018.
1023   50.   Q. Liu, A. Zhang, R. Wang, Q. Zhang and D. Cui, *Nano-micro letters*, 2021, **13**, 1-53.
1024   51.   Z. Karimzadeh, M. Mahmoudpour, M. d. l. Guardia, J. Ezzati Nazhad Dolatabadi and A. Jouyban,
1025   *TrAC Trends in Analytical Chemistry*, 2022, **152**, 116622.
1026   52.   Z. Karimzadeh, M. Mahmoudpour, E. Rahimpour and A. Jouyban, *RSC advances*, 2024, **14**, 9571-
1027   9586.
1028   53.   Z. Karimzadeh, A. Jouyban, A. Ostadi, A. Gharakhani and E. Rahimpour, *Analytica Chimica Acta*,
1029   2022, **1227**, 340252.
1030   54.   X. Zhang, G. Li, D. Wu, X. Li, N. Hu, J. Chen, G. Chen and Y. Wu, *Biosensors and Bioelectronics*,
1031   2019, **137**, 178-198.
1032   55.   X. Huang, S. Zhang, Y. Tang, X. Zhang, Y. Bai and H. Pang, *Coordination Chemistry Reviews*, 2021,
1033   **449**, 214216.
1034   56.   W. He, Z. Li, S. Lv, M. Niu, W. Zhou, J. Li, R. Lu, H. Gao, C. Pan and S. Zhang, *Chemical Engineering
1035   Journal*, 2021, **409**, 128274.
1036   57.   K. Zhang, K. Dai, R. Bai, Y. Ma, Y. Deng, D. Li, X. Zhang, R. Hu and Y. Yang, *Chinese Chemical
1037   Letters*, 2019, **30**, 664-667.
1038   58.   Z. Sun, M. Wang, J. Fan, R. Feng, Y. Zhou and L. Zhang, *Advanced Composites and Hybrid
1039   Materials*, 2021, **4**, 1322-1329.
1040   59.   Y. Su, M. Lu, R. Su, W. Zhou, X. Xu and Q. Li, *Chinese Chemical Letters*, 2022, **33**, 2573-2578.
1041   60.   L. Zheng, F. Wang, C. Jiang, S. Ye, J. Tong, P. Dramou and H. He, *Coordination Chemistry Reviews*,
1042   2022, **471**, 214760.
1043   61.   X. Niu, B. Liu, P. Hu, H. Zhu and M. Wang, *Biosensors*, 2022, **12**, 251.
1044   62.   H. Deng, Y. Zhang, X. Cai, Z. Yin, Y. Yang, Q. Dong, Y. Qiu and Z. Chen, *Small*, 2024, **20**, 2306155.
1045   63.   Z. Wang, M. Li, H. Bu, D. S. Zia, P. Dai and J. Liu, *Materials Chemistry Frontiers*, 2023, **7**, 3625-
1046   3640.
1047   64.   M.-L. Ye, Y. Zhu, Y. Lu, L. Gan, Y. Zhang and Y.-G. Zhao, *Talanta*, 2021, **230**, 122299.
1048   65.   Y. Song, K. Qu, C. Zhao, J. Ren and X. Qu, *Advanced Materials*, 2010, **22**, 2206-2210.
1049   66.   Z. Lyu, J. Zhou, S. Ding, D. Du, J. Wang, Y. Liu and Y. Lin, *TrAC Trends in Analytical Chemistry*,
1050   2023, 117280.
1051   67.   X. Zhang, C. Sun, R. Li, X. Jin, Y. Wu and F. Fu, *Analytical Chemistry*, 2023, **95**, 5024-5033.
1052   68.   H. Li, M. Sun, H. Gu, J. Huang, G. Wang, R. Tan, R. Wu, X. Zhang, S. Liu and L. Zheng, *Small*, 2023,
1053   **19**, 2207036.
1054   69.   M. Comotti, C. Della Pina, R. Matarrese and M. Rossi, *Angewandte Chemie International Edition*,
1055   2004, **43**, 5812-5815.
1056   70.   Y. Peng, M. Huang, L. Chen, C. Gong, N. Li, Y. Huang and C. Cheng, *Nano Research*, 2022, **15**,
1057   8783-8790.
1058   71.   M. Ren, Y. Zhang, L. Yu, L. Qu, Z. Li and L. Zhang, *Talanta*, 2023, **255**, 124219.
1059   72.   X. Zhou, M. Wang, J. Chen and X. Su, *Talanta*, 2022, **245**, 123451.
1060   73.   S. Khajir, Z. Karimzadeh, M. Khoubnasabjafari, V. Jouyban-Gharamaleki, E. Rahimpour and A.
1061   Jouyban, *Journal of Pharmaceutical and Biomedical Analysis*, 2023, **223**, 115141.
1062   74.   S. Singh, *Frontiers in chemistry*, 2019, **7**, 46.
1063   75.   S. Singh, *International Journal of Biological Macromolecules*, 2024, 129374.
1064   76.   D. Mehta, P. Sharma and S. Singh, *Colloids and Surfaces B: Biointerfaces*, 2023, **231**, 113531.
1065   77.   M. S. Lord, J. F. Berret, S. Singh, A. Vinu and A. S. Karakoti, *Small*, 2021, **17**, 2102342.

78. A. K. Singh, K. Bijalwan, N. Kaushal, A. Kumari, A. Saha and A. Indra, *ACS Applied Nano Materials*, 2023, **6**, 8036-8045.

79. M. Zhang, Y. Wang, N. Li, D. Zhu and F. Li, *Biosensors and Bioelectronics*, 2023, **237**, 115554.

80. M. Jia, F. Xu, F. Zhai, X. Yu and M. Du, *Journal of Colloid and Interface Science*, 2024, **653**, 1805-1816.

81. C. P. Liu, T. H. Wu, C. Y. Liu, K. C. Chen, Y. X. Chen, G. S. Chen and S. Y. Lin, *Small*, 2017, **13**, 1700278.

82. S. Guo, Y. Han and L. Guo, *Catalysis Surveys from Asia*, 2020, **24**, 70-85.

83. Z. Wang, X. Shen, X. Gao and Y. Zhao, *Nanoscale*, 2019, **11**, 13289-13299.

84. R. Zhang, B. Xue, Y. Tao, H. Zhao, Z. Zhang, X. Wang, X. Zhou, B. Jiang, Z. Yang and X. Yan, *Advanced Materials*, 2022, **34**, 2205324.

85. W. Yang, X. Yang, L. Zhu, H. Chu, X. Li and W. Xu, *Coordination Chemistry Reviews*, 2021, **448**, 214170.

86. A. Casu, M. Camardo Leggieri, P. Toscano and P. Battilani, *Comprehensive Reviews in Food Science and Food Safety*, 2024, **23**, e13323.

87. M.-H. Moosavy, M. Hasanzadeh, J. Soleymani and A. Mokhtarzadeh, *Analytical methods*, 2019, **11**, 3910-3919.

88. Y. Zhang, X. Chen, X. Xie, D. Li, Y. Fan, B. Huang and X. Yang, *Current Analytical Chemistry*, 2024, **20**, 242-254.

89. Z. Xue, Y. Zhang, W. Yu, J. Zhang, J. Wang, F. Wan, Y. Kim, Y. Liu and X. Kou, *Analytica chimica acta*, 2019, **1069**, 1-27.

90. C. Peng, R. Pang, J. Li and E. Wang, *Advanced Materials*, 2024, **36**, 2211724.

91. X. Zhao, Q. Li, H. Li, Y. Wang, F. Xiao, D. Yang, Q. Xia and Y. Yang, *Food Chemistry*, 2023, **424**, 136443.

92. W. Lai, J. Guo, Y. Wang, Y. Lin, S. Ye, J. Zhuang and D. Tang, *Talanta*, 2022, **247**, 123546.

93. L. Wu, M. Zhou, Y. Wang and J. Liu, *Journal of hazardous materials*, 2020, **399**, 123154.

94. W. Jiang, Q. Yang, H. Duo, W. Wu and X. Hou, *Food Chemistry*, 2024, 138917.

95. S. Huang, W. Lai, B. Liu, M. Xu, J. Zhuang, D. Tang and Y. Lin, *Spectrochimica Acta Part A: Molecular and Biomolecular Spectroscopy*, 2023, **284**, 121782.

96. N. Ullah, T. A. Bruce-Tagoe, G. A. Asamoah and M. K. Danquah, *International Journal of Molecular Sciences*, 2024, **25**, 5959.

97. S. Ganguly and S. Margel, *Talanta Open*, 2023, 100243.

98. X. Tan, K. Kang, R. Zhang, J. Dong, W. Wang and W. Kang, *Sensors and Actuators B: Chemical*, 2024, **412**, 135854.

99. X. Cai, M. Liang, F. Ma, Z. Zhang, X. Tang, J. Jiang, C. Guo, S. R. Mohamed, A. A. Goda and D. H. Dawood, *Food Chemistry*, 2022, **377**, 131965.

100. T. Bu, P. Jia, X. Sun, Y. Liu, Q. Wang and L. Wang, *Sensors and Actuators B: Chemical*, 2020, **320**, 128440.

101. X. Zhu, J. Tang, X. Ouyang, Y. Liao, H. Feng, J. Yu, L. Chen, Y. Lu, Y. Yi and L. Tang, *Journal of Hazardous Materials*, 2024, **465**, 133178.

102. Y. Fan, D. Li, X. Xie, Y. Zhang, L. Jiang, B. Huang and X. Yang, *Microchemical Journal*, 2024, **197**, 109842.

103. X. Zhang, M. C. Wasson, M. Shayan, E. K. Berdichevsky, J. Ricardo-Noordberg, Z. Singh, E. K. Papazyan, A. J. Castro, P. Marino and Z. Ajoyan, *Coordination chemistry reviews*, 2021, **429**, 213615.

104. P. Li, R. C. Klet, S.-Y. Moon, T. C. Wang, P. Deria, A. W. Peters, B. M. Klahr, H.-J. Park, S. S. Al-Juaid and J. T. Hupp, *Chemical communications*, 2015, **51**, 10925-10928.

105. S. Zhang, H. Li, Q. Xia, D. Yang and Y. Yang, *Journal of Food Science*, 2024.

Analytical Methods Accepted Manuscript

Analytical Methods Accepted Manuscript

106.   S. Peng, K. Li, Y.-x. Wang, L. Li, Y.-H. Cheng and Z. Xu, *Analytical Biochemistry*, 2022, **655**, 114829.

107.   C. Jiang, L. Lan, Y. Yao, F. Zhao and J. Ping, *TrAC Trends in Analytical Chemistry*, 2018, **102**, 236-249.

108.   Y. Alhamoud, D. Yang, S. S. F. Kenston, G. Liu, L. Liu, H. Zhou, F. Ahmed and J. Zhao, *Biosensors and Bioelectronics*, 2019, **141**, 111418.

109.   Q. Zhao, Z. Yan, C. Chen and J. Chen, *Chemical reviews*, 2017, **117**, 10121-10211.

110.   L. Gao, K. Fan and X. Yan, *Nanozymology: Connecting Biology and Nanotechnology*, 2020, 105-140.

111.   L. Huang, K. Chen, W. Zhang, W. Zhu, X. Liu, J. Wang, R. Wang, N. Hu, Y. Suo and J. Wang, *Sensors and Actuators B: Chemical*, 2018, **269**, 79-87.

112.   J. M. Gonçalves, L. V. de Faria, A. B. Nascimento, R. L. Germscheidt, S. Patra, L. P. Hernández-Saravia, J. A. Bonacin, R. A. Munoz and L. Angnes, *Analytica Chimica Acta*, 2022, **1233**, 340362.

113.   Q. Liu, S. Xin, X. Tan, Q. Yang and X. Hou, *Microchimica Acta*, 2023, **190**, 364.

114.   M. K. Masud, J. Kim, M. M. Billah, K. Wood, M. J. Shiddiky, N.-T. Nguyen, R. K. Parsapur, Y. V. Kaneti, A. A. Alshehri and Y. G. Alghamidi, *Journal of materials chemistry B*, 2019, **7**, 5412-5422.

115.   F. Tian, J. Zhou, B. Jiao and Y. He, *Nanoscale*, 2019, **11**, 9547-9555.

116.   H. Zhu, Z. Quan, H. Hou, Y. Cai, W. Liu and Y. Liu, *Analytica Chimica Acta*, 2020, **1132**, 101-109.

117.   L. Zhao, H. Guo, H. Chen, B. Zou, C. Yang, X. Zhang, Y. Gao, M. Sun and L. Wang, *Bioengineering*, 2022, **9**, 684.

118.   H. kholafazad Kordasht, S. Hassanpour, B. Baradaran, R. Nosrati, M. Hashemzaei, A. Mokhtarzadeh and M. de la Guardia, *Biosensors and Bioelectronics*, 2020, **165**, 112403.

119.   O. D. Hendrickson, E. A. Zvereva, V. G. Panferov, O. N. Solopova, A. V. Zherdev, P. G. Sveshnikov and B. B. Dzantiev, *Biosensors*, 2022, **12**, 1137.

120.   Y. Zhao, L. Li, R. Ma, L. Wang, X. Yan, X. Qi, S. Wang and X. Mao, *Analytica Chimica Acta*, 2021, **1173**, 338710.

121.   X. Qi, L. Li, X. Yan, Y. Zhao, L. Wang, R. Ma, S. Wang and X. Mao, *Journal of Ocean University of China*, 2022, **21**, 1343-1350.

122.   S. Wang, Y. Zhao, R. Ma, W. Wang, L. Zhang, J. Li, J. Sun and X. Mao, *Food Chemistry*, 2023, **401**, 134053.

123.   L. Li, R. Ma, Y. Zhao, L. Wang, S. Wang and X. Mao, *Talanta*, 2022, **246**, 123534.

124.   F. Cui, Z. Zhou and H. S. Zhou, *Sensors*, 2020, **20**, 996.

125.   J. Marfà, R. Pupin, M. Sotomayor and M. Pividori, *Analytical and Bioanalytical Chemistry*, 2021, **413**, 6141-6157.

126.   L. Wu, Y. Li, Y. Han, X. Liu, B. Han, H. Mao and Q. Chen, *Journal of Food Composition and Analysis*, 2024, **130**, 106190.

127.   C. H. Cho, J. H. Kim, N. S. Padalkar, Y. V. M. Reddy, T. J. Park, J. Park and J. P. Park, *Biosensors and Bioelectronics*, 2024, **255**, 116269.

128.   C. Hernández-Cortez, I. Palma-Martínez, L. U. Gonzalez-Avila, A. Guerrero-Mandujano, R. C. Solís and G. Castro-Escarpulli, *Poisoning: From specific toxic agents to novel rapid and simplified techniques for analysis*, 2017, **33**.

129.   R. Gupta, N. Raza, S. K. Bhardwaj, K. Vikrant, K.-H. Kim and N. Bhardwaj, *Journal of hazardous materials*, 2021, **401**, 123379.

130.   K. Ren, M. Duan, T. Su, D. Ying, S. Wu, Z. Wang and N. Duan, *Talanta*, 2024, **270**, 125636.

131.   H. Liang, H. Liu, H. Lin, G. Ning, X. Lu, S. Ma, F. Liu, H. Zhao and C. Li, *Food Science and Human Wellness*, 2024, **13**, 2025-2035.

132.   X. Cai, Y. Luo, C. Zhu, D. Huang and Y. Song, *Sensors and Actuators B: Chemical*, 2022, **367**, 132066.

1161   133.   Y. Xing, F. Yasinjan, S. Sun, J. Yang, Y. Du, H. Zhang, Y. Liang, H. Geng, Y. Wang and J. Sun, *Nano*
1162   *Today*, 2024, **57**, 102386.
1163   134.   D. Li, T. Fan and X. Mei, *Nanoscale*, 2023, **15**, 15885-15905.
1164   135.   Q. Lu, Q. Li, Y. An, X. Duan, R. Zhao, D. Zhao and S. An, *Journal of Cleaner Production*, 2022, **376**,
1165   134117.
1166   136.   M. Tudi, H. Daniel Ruan, L. Wang, J. Lyu, R. Sadler, D. Connell, C. Chu and D. T. Phung,
1167   *International journal of environmental research and public health*, 2021, **18**, 1112.
1168   137.   M. Song, University of Nevada, Reno, 2022.
1169   138.   N. K. V. Leitner, in *Advanced oxidation processes for water treatment: fundamentals and*
1170   *applications*, IWA Publishing, 2017, pp. 429-460.
1171   139.   Z. A. Mohamed, Y. Mostafa, S. Alamri, M. Hashem and S. Alrumman, 2022.
1172   140.   X. Yang, J. Pan, J. Hu, S. Zhao and K. Cheng, *Chemical Engineering Journal*, 2023, **467**, 143381.
1173   141.   W. Jiang, Q. Yang, H. Duo, W. Wu and X. Hou, *Food Chemistry*, 2024, **447**, 138917.
1174   142.   S. Zhang, H. Li, Q. Xia, D. Yang and Y. Yang, *Journal of Food Science*, 2024, **89**, 3618-3628.
1175   143.   R. Zhang, X. Yan and K. Fan, *Accounts of Materials Research*, 2021, **2**, 534-547.
1176   144.   Y. Chong, Q. Liu and C. Ge, *Nano Today*, 2021, **37**, 101076.

1177

1178

1179

1180

1181

1182

1183

1184

1185

1186

1187

Analytical Methods Accepted Manuscript

Data availability

No data was used for the research described in the article.

Analytical Methods Accepted Manuscript